Adaptive Response to Fluconazole in *Candida parapsilosis*: Ergosterol Pathway Mutations, Gene Expressions, and Metabolomic Shifts

by

Kübra Çam

A Dissertation Submitted to the
Graduate School of Health Sciences
in Partial Fulfillment of the Requirements for
the Degree of

Master of Science

in

Medical Microbiology

April 17, 2024

Adaptive Response to Fluconazole in *Candida parapsilosis*: Ergosterol Pathway Mutations, Gene Expressions, and Metabolomic Shifts

Koç University

Graduate School of Health Sciences

This is to certify that I have examined this copy of a master's thesis by

Kübra Çam

and have found that it is complete and satisfactory in all respects,

and that any and all revisions required by the final

examining committee have been made.

Committee Members:

Asst .Prof. Dr. Özlem Doğan (Advisor)

Prof. Dr. Füsun Can

Prof. Dr. Dolunay Gülmez Kıvanç

Assoc. Prof. Dr. Mert Ahmet Kuşkucu

Asst. Prof. Dr. Çağdaş Dağ

Date: April 17, 2024

ABSTRACT

Adaptive Response to Fluconazole in *Candida parapsilosis*: Ergosterol Pathway Mutations, Gene Expressions, and Metabolomic Shifts

Kübra Çam

Master of Science in Medical Microbiology

April 17, 2024

Candida parapsilosis complex is the second most common cause of bloodstream infection among Candida species both in our country and in many centers in Southern Europe and become a major health-care problem due to the increasing antifungal resistance. Azoles, an important group of antifungal drugs are bind to lanosterol demethylase and inhibit the enzyme. Resistance is usually associated with point mutations in the ERG11 gene and ERG3 genes which are play role in ergosterol biosynthesis. This study aims to analyze the effects of fluconazole on *C. parapsilosis* cells in metabolomic, transcriptomic and genomic level especially focusing on the critical steps in ergosterol synthesis pathway.

In this study, 15 fluconazole non-susceptible *C.parapsilosis* isolates are included. Analysis of the resistance profile is performed with broth microdilution test according to Clinical and Laboratory Standards Institute (CLSI) guidelines. Fluconazole non-susceptible isolates are treated with the 0.5 Minimum Inhibitory Concentration (MIC) and 1 MIC of fluconazole and the mRNA expression level changes are measured with quantitative real-time polymerase chain reaction (qRT-PCR) method. Effects of fluconazole on the metabolomic profiles of *C.prarapsilosis* cells are examined with Nucleic Magnetic Resonance Spectroscopy (NMR).

Sanger sequence analysis showed that 10/15 (66%) of the isolates were harboring Y132F mutations in ERG11 gene and all of them were carrying missense mutation (C825T) in ERG3 gene. Although, an increase in ERG11 mRNA expression levels is observed regardless of the mutation type, some of the selected isolates behaved controversial under fluconazole exposure. Together with all isolates, especially K478 had a decreasing ERG11 mRNA expression level trend under higher fluconazole concentration. Even if the highest ERG3 and UPC2 mRNA expression levels were observed in K478, the same decreasing trend were also detected under higher fluconazole concentrations in these genes. According to metabolomic analysis results, under the fluconazole exposure, the metabolic pathways most significantly altered are :1) alanine, aspartate, and glutamate metabolism; 2) arginine and proline metabolism, 3) homocysteine, methionine metabolism and 4) arabinitol metabolism. These metabolomic changes observed in our study, we assumed that they might be related with two important biochemical processes which are nitrogen assimilation and oxidative stress responses.

In conclusion, in drug-resistant *C. parapsilosis* isolates, the response to fluconazole exposure in terms of mRNA expression of ergosterol biosynthesis enzyme genes is strain-specific, clearly indicating that besides point mutations in the enzyme genes of ergosterol synthesis and control, there are numerous different regulations. These regulations lead to a wide range of metabolomic changes within the cell, while a common metabolic response is formed in almost all isolates to neutralize the toxic effect of fluconazole and ensure survival. A detailed in-depth investigation of this survival response will uncover new drug targets in the future.

Keywords: *C.parapsilosis,* azole resistance*,* ERG11 gene, ERG3 gene,UPC2 gene, quantitative real-time PCR(qRT-PCR), Sanger sequence, NMR spectroscopy

ÖZETÇE

Candida parapsilosis'de Flukonazole Uyum Yanıtı: Ergosterol Yolağı Mutasyonları, Gen Ekspresyonları ve Metabolomik Değişimler

Kübra Çam

Medikal Mikrobiyoloji, Yüksek Lisans

17 Nisan 2024

Candida parapsilosis kompleks, ülkemizde ve Güney Avrupa'daki birçok merkezde *Candida* türleri arasında kan dolaşımı enfeksiyonunun ikinci en sık nedeni olup, antifungal direncin artması nedeniyle önemli bir sağlık sorunu haline gelmektedir. Antifungal ilaçların önemli bir grubu olan azoller, lanosterol demetilaza bağlanarak bu enzimi inhibe eder. Direnç genellikle ergosterol biyosentezinde rol oynayan ERG11 ve ERG3 genlerindeki nokta mutasyonlarla ilişkilidir. Bu çalışmanın amacı flukonazolün *C. parapsilosis* izoları üzerindeki etkilerini metabolomik, transkriptomik ve genomik düzeyde incelemektir.

Bu çalışmaya 15 flukonazol dirençli *C.parapsilosis* izolatı dahil edilmiştir. Direnç profilinin analizi, Klinik ve Laboratuvar Standartları Enstitüsü (CLSI) kılavuzlarına göre sıvı mikrodilüsyon testiyle gerçekleştirilmiştir. Flukonazole duyarlı olmayan izolatlar, flukonazolün 0.5 Minimum İnhibitör Konsantrasyonu (MIK) ve 1 MIK konsantrasyonuna maruz bırakılarak mRNA ekspresyon seviyesi değişiklikleri, kantitatif gerçek zamanlı polimeraz zincir reaksiyonu (qRT-PCR) ile ölçülmüştür. Flukonazolün *C.prarapsilosis* hücrelerinin metabolomik profilleri üzerindeki etkileri Nükleik Manyetik Rezonans Spektroskopisi (NMR) ile incelenmiştir.

Sanger dizi analizi sonuçları izolatların 10/15'inin (%66) ERG11 geninde Y132F mutasyonu taşıdığını ve hepsinin ERG3 geninde missense mutasyon (C825T) taşıdığını göstermiştir. Mutasyon tipine bakılmaksızın ERG11 mRNA ekspresyonunda bir artış gözlenmesine rağmen, seçilen izolatlardan bazıları flukonazol maruziyeti altında farklı davranışlar sergilemiştir. Tüm izolatlarla birlikte özellikle K478'in daha yüksek flukonazol konsantrasyonu altında ERG11 mRNA ekspresyon düzeyi azalması eğilimi gösterdiği görülmüştür. En yüksek ERG3 ve UPC2 mRNA ekspresyon seviyeleri K478'de gözlenmiş olsa da, aynı azalma eğilimi bu genlerdeki yüksek flukonazol konsantrasyonlarında da tespit edilmiştir. Metabolomik analiz sonuçlarına göre, flukonazol maruziyeti altında en belirgin şekilde değişen metabolik yollar 1) alanin, aspartat ve glutamat metabolizması; 2) arginin ve prolin metabolizması, 3)homosistein, metionin metabolizması ve 4) arabinitol metabolizmasıdır. Çalışmamızda gözlenen bu metabolomik değişikliklerin, nitrojen asimilasyonu ve oksidatif stres tepkileri olan iki önemli biyokimyasal süreçle ilişkili olduğu düşünülmektedir.

Sonuç olarak, ilaca dirençli *C. parapsilosis* izolatlarında, ergosterol biyosentezi ile ilişkili enzim genlerinin mRNA ekspresyonu açısından flukonazol maruziyetine verilen yanıt suşa özgüdür. Bu durum, ergosterol sentezi yolağı ve kontrolü ile ilişkili enzimleri kodlayan genlerindeki nokta mutasyonlarının yanı sıra, farklı hücre içi düzenlemelerin olduğunu göstermektedir. Bu düzenlemeler hücre içinde çok çeşitli metabolomik değişikliklere yol açarken, hemen hemen tüm izolatlarda flukonazolün toksik etkisini nötralize etmek ve hayatta kalmayı sağlamak için ortak bir metabolik yanıt oluştuğu

gözlenmektedir. Bu hayatta kalma stratejisinin ayrıntılı ve derinlemesine araştırılması, gelecekte yeni ilaç hedeflerini ortaya çıkarılmasına katkı sunacaktır.

Anahtar kelimeler: *C.parapsilosis*, azol direnci, ERG11 geni, ERG3 geni, UPC2 geni, kantitatif gerçek zamanlı PCR(qRT-PCR), Sanger dizileme, NMR spektroskopisi

ACKNOWLEDGEMENTS

Firstly, I would like to express my sincere gratitude to my thesis advisor **Asst.Prof. Özlem Doğan**. I am grateful to work under supervision of Özlem Doğan, who taught me the ways of being a researcher throughout my master's journey and inspired me with her human-centered philosophy of life. She always cared about my opinions, listened to me with great understanding and empathy on many issues, and gave great advices. I feel lucky to have the opportunity to learn from her experiences and her great leadership.

Secondly. I would like to thank **Prof. Dr. Füsun Can**, for her valuable contributions to my thesis project and for generously sharing her experiences with us in weekly meetings. She inspired me with her understanding of what it means to be both a team member and a researcher.

I would like to thank **Prof. Dr. Önder Ergönül**, who I think is a great leader, who always has a smile on his face.

I would also like to thank **Assoc. Prof Mert Ahmet Kuşkucu**, for his support my thesis. Whenever I ask for his guidance, he always eager to share his valuable informations and advices. I would like to thank **Asst. Prof. Çağdaş Dağ**, for this endless support during the most challenging part of my thesis with his expertise in the area, he generously shared his guidance along the way, and helped me learn about a new topic.

I am grateful to **my great colleagues at KUISCID** for the support they gave me in any time and for helping to overcame difficulties together. Learning to be a team member with them was a unique experience.

I would like to chance to thank my dear friend **Betül Durmuş** for being with me throughout every period of my life with her love and support and for her constant encouragement along the way. I would also like to thank **Remzi Can Alabalık** for being there for me in my anxious moments, for his endless support, and for the coffees he prepared.

Last, but not least, I am sincerely grateful to my **loving parents and sisters**. I feel very lucky that they gave me their love, support, and encouragement when I wanted to begin on this journey.

TABLE OF CONTENTS

LIST OF TABLES

LIST OF FIGURES

ABBREVIATIONS

CLSI	Clinical and Laboratory Standards Institute
MIC	Minimum Inhibitory Concentration
qRT-PCR	Quantitative Real-time Polymerase Chain Reaction
NMR	Nucleic Magnetic Resonance Spectroscopy
CVCs	Central Venous Catheters
Mbp	Megabase pair
FLC	Fluconazole
PSC	Posaconazole
VRC	Voriconazole
HPLC-MS	High-Performance Liquid Chromatography Mass Spectrometry
GC-MS	Gas Chromatography-Mass Spectrometry
UPC2	Sterol Uptake Control Protein 2
MALDI-TOF MS	Matrix-Assisted Laser Desorption Ionization-Time-Of-Flight Mass Spectrometry
KUISCID	Koc University-Is Bank Center for Infectious Diseases
PBS	Phosphate Buffer Saline
CFU	Colony-Forming Units
PCR	Polymerase Chain Reaction
OD	Optical Density
CT	Cycle Threshold
ACT1	Actin
PLS	Partial Least Squares
PLS-DA	Partial Least-Squares Discriminant Analysis
VIP	Variable Importance in Projection
CBP	Clinical Breakpoints
ECV	Epidemiological Cut-off Values
AmB	Amphotericin B
SAM	S-adenosyl methionin
DNA	Deoxyribonucleic acid
RNA	Ribonucleic acid
NF	Nuclease Free
WHO	World Health Organisation

Chapter 1:
INTRODUCTION

Bloodstream infections caused by *Candida* species (candidemias) are associated with high morbidity and mortality, especially in immunocompromised patients. In recent years, the rapid increase in this patient population (received organ or bone marrow transplant, diabetic, receiving chemotherapy, corticosteroid and broad-spectrum antibiotic treatment, etc.) has also led to an increase in the number of hosts susceptible to fungal infections (Benedict et al., 2017).

Candida species characterized by their 3 to 5 um size oval yeastlike form, buds or blastoconidia production. Besides *Candida glabrata* other *Candida* species produce pseudohyphae and true hyphae (Murray et al., 2020). Glucans and mannans, as well as proteins and chitin, are some of the several substances that make up the cell wall of *Candida*, which gives the cell its structural integrity and defense (Garcia-Rubio et al., 2019).

Although the most common cause of candidemia is *Candida albicans*, recent epidemiological studies draw attention to changes in the species-level distribution of *Candida* species that cause bloodstream infections. While *C.albicans* remains the most frequently isolated species, the incidence of non-albicans *Candida* species is increasing worldwide. *Candida parapsilosis* is one of them that is particularly significant because it can develop tenacious biofilms on central venous catheters (CVCs) and other medical implants (Tóth et al., 2019).Many factors affect the distribution of *Candida* species, such as patient age, antifungal exposure, comorbidities, geographic region, and hospital infection control policies (Guinea, 2014).

1.1 Candida parapsilosis

C. parapsilosis complex is the second most common type that causes bloodstream infection among *Candida* species both in our country and in many centers in Southern Europe(Arikan-Akdagli et al., 2019; Soulountsi et al., 2021). In the *C. parapsilosis* complex, together with *C. parapsilosis sensu stricto*, which gives the species its name, there are other cryptic species, *Candida orthopsilosis* and *Candida metapsilosis*, these two species occupy 2% of the whole complex and are rarely isolated (Gomez-Lopez). et

al., 2008). In a study performed in Turkey, clinical *C. parapsilosis* complex strain is identified and found that majority of the isolates were *C.parapsilosis* sensu stricto. Among 42 of the isolates one of them identified as *C. orthopsilosis* three of them identified as *C. metapsilosis*. Also, antifungal susceptibility profile is compared and they did not differ significantly from *C. parapsilosis sensu stricto*, despite the fact that the number of *C. metapsilosis* and *C. orthopsilosis* isolates remained low (Tosun et al., 2013).

1.2 Taxonomy

The specific taxonomy of *C. parapsilosis* has been described as: "Superkingdom Eukaryota, kingdom Fungi, subkingdom Dikarya, phylum Ascomycota, clade saccharomyceta, subphylum Saccharomycotina, class Saccharomycetes, order Saccharomycetales, family Debaryomycetaceae, clade CUG-Ser1 clade, genus *Candida*, species parapsilosis(Schoch et al., 2020).

1.3 General Properties

C. parapsilosis was first discovered in 1928 and its phylogenetic classification has encountered numerous modifications since then. Initially identified as *Monilia parapsilosis*, it was discovered in the feces of a patient in Puerto Rico who had diarrhea. It was given the name *C. parapsilosis* in 1932. The existence of the *C. parapsilosis* complex, which consists of the three different species *C. parapsilosis sensu stricto*, *C. orthopsilosis*, and *C. metapsilosis*, was established in 2005 by Tavanti et al. by using multilocus sequence typing (Branco et al., 2023; Tavanti et al., 2005).

C. parapsilosis is diploid with eight chromosome pairs, these chromosome pairs are between 0.9 to 3.0 Megabase pair (Mbp), genome size is about 13 Mbp (Tóth et al., 2019).*C. parapsilosis* is a widely dispersed microorganism that can be found in the natural environment, such as soil, seawater, and plants, as well as in a variety of non-human sources, such as domestic animals, insects, mucosal surfaces, skin, and nails, where it is a part of the microbiome of human and mammals (Branco et al., 2023; van Asbeck et al., 2009).

C. parapsilosis colonizes the central venous catheters of patients receiving long-term health care due to slime and biofilm formation and causes bloodstream infections by originating from there. Patients with compromised immune systems, such as those living

with HIV or those undergoing surgery, particularly gastrointestinal surgery, are at high risk of developing *C. parapsilosis* infections In addition, individuals who have long-term central venous catheters or implants are extremely vulnerable since *C. parapsilosis* is able to rapidly build biofilms on these devices and attach themselves to them. As these biofilms develop, the effectiveness of antifungal medications is drastically decreased, it causes serious risk for the host's life. (Branco et al., 2023; Cuéllar-Cruz et al., 2012).

Unlike other Candida species, *C. parapsilosis* also colonizes the hands of healthcare personnel, patient rooms and the devices, and causes outbreaks in hospitals. In the reported studies, it has been observed that *C. parapsilosis* infects newborns as well as adult patients and creates alarming outbreaks in neonatal intensive care units (Tóth et al., 2019). According to previous publications in the literature, *C. parapsilosis*, which was previously considered a benign species due to its lower mortality rate compared to other Candida species, has become a major problem in clinics due to the increasing antifungal resistance problem in recent years.

1.4 Epidemiology

Geographical location, hospital infection control policies, patients' predisposing illnesses, patient age, antifungal exposure, and geographic region all have an impact on the distribution of *C.parapsilosis* that cause candidemia(Guinea, 2014).

C. parapsilosis is the second most commonly isolated species among the species that cause candidemia both in our country and in Southern Europe such as Spain, Italy, Portugal, Greece and Latin America countries such as Brazil, Argentina. In Brazil, Argentina, Peru, Spain, Russia, and China more than 20% of *Candida* species found in blood cultures defined as *C. parapsilosis* , and more than 30% in Turkey, Greece, Croatia, Romania, South Africa, Nigeria, and Paraguay as well (Figure *1.1*)(Daneshnia et al., 2023; Faria-Ramos et al., 2014; Guinea, 2014; Nucci et al., 2013).

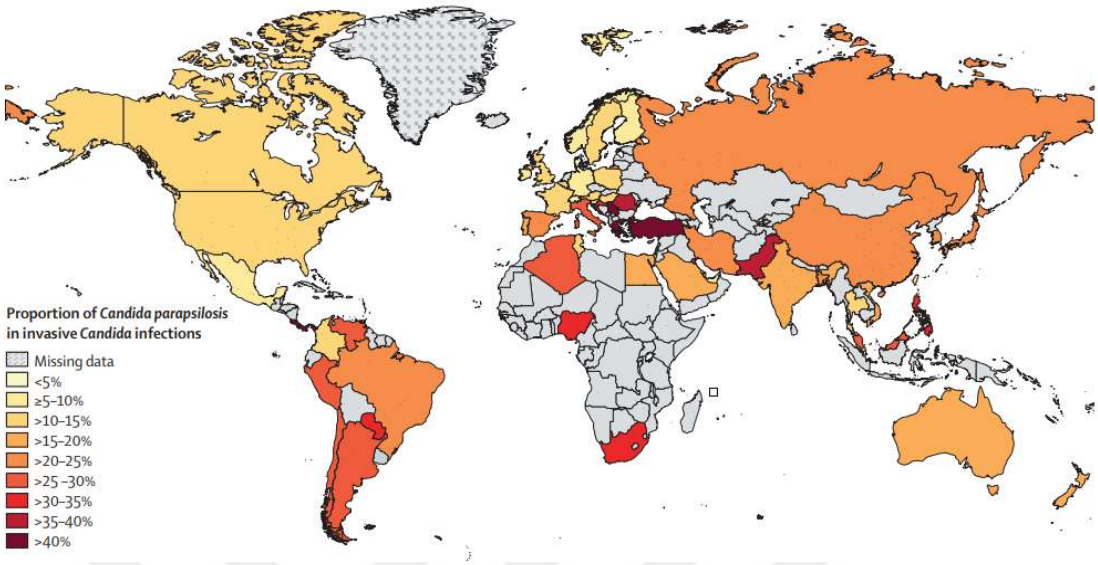

Figure 1.1:Prevelance of *Candida parapsilosis* in invasive Candida infections (Daneshnia et al., 2023)

1.5 Treatment

Three main groups of antifungal drugs are currently used in the treatment of candidemia: azoles, echinocandins and liposomal amphotericin B. According to the isolated fungus' susceptibility profile to antifungal treatments, azole group therapies are recommended primarily because they are more affordable than these medications and have a more limited range of adverse effects (Pappas et al., 2016). Fluconazole (FLC), voriconazole (VRC), posaconazole (PSC), itraconazole, and isavuconazole are among the azoles that have received clinical approval. Azoles primarily battle candidiasis by fungistatic action (Robbins et al., 2017).

1.6 Azole resistance in Candida parapsilosis

Candida species have developed various resistance strategies against the effect of azole drugs on fungal cells. High usage rates of azole drugs in clinics, long-term prophylactic use of fluconazole in some patient groups, and the fungistatic nature of the drug cause selective pressure among *Candida* species and create resistance problems. In as study performed in our country, fluconazole susceptibility pattern between 1991-2017 is analysed and they revealed increasing fluconazole resistance rates (Demirci-Duarte et al., 2021). Many mechanisms that cause resistance in *Candida* species have been

described. Some of these mechanisms are related to the target enzyme, while others are related to the discharge of the drug, such as efflux pumps (Bhattacharya et al., 2020).

Different molecular mechanisms that are related with resistance in *Candida* species are reported in the literature(Figure *1.2*).

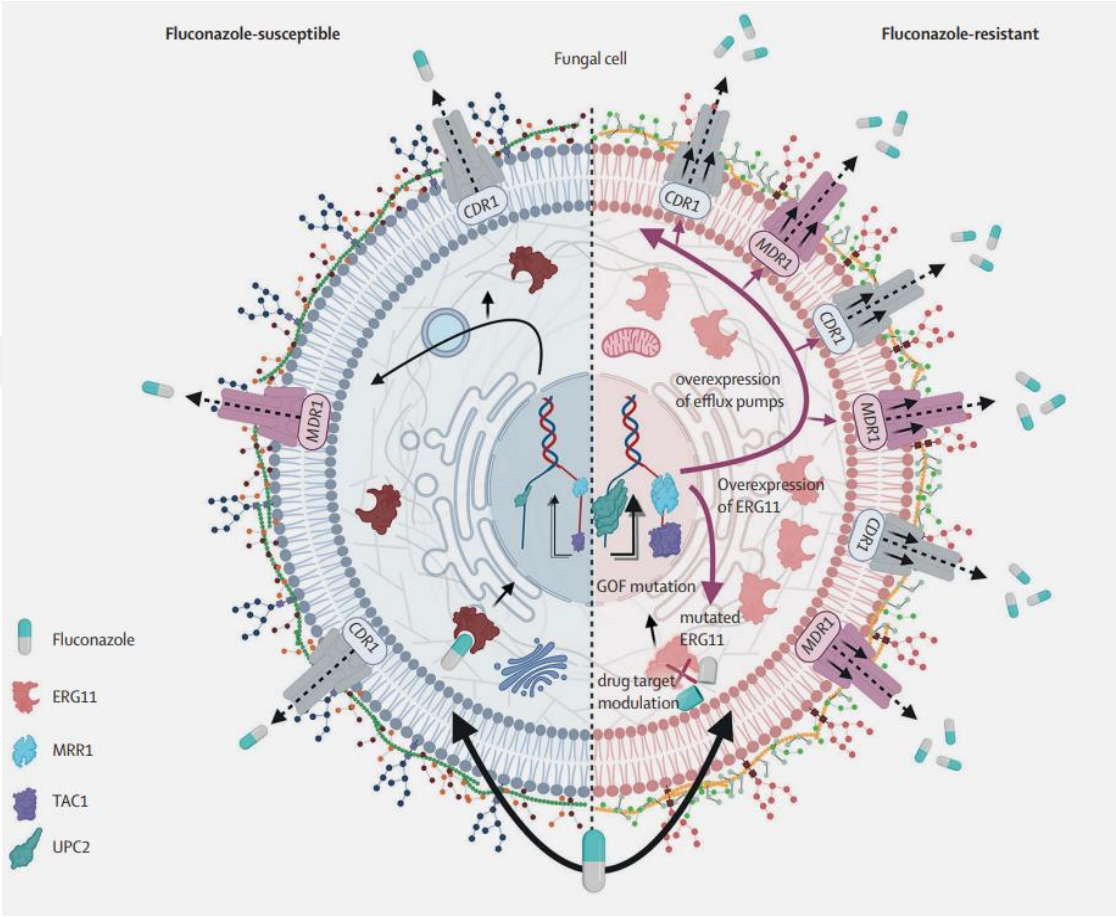

Figure 1.2:Main mechanisms that promoting azole resistance in *Candida* species(Daneshnia et al., 2023)

a) Ergosterol synthesis related resistance mechanisms:

Dominant mechanism in azole resistance is target alterations, ERG11p substitutions. Azoles function by preventing the lanosterol 14-alpha-demethylase enzyme, which is produced by the ERG11 gene. The structure of the enzyme may alter as a result of mutations in this gene, decreasing the azole–target binding affinity for azole drugs.

ERG3 gene plays crucial role in the production of ergosterol which is the main component for the integrity of cell membranes, even though they are rare, mutations in ERG3 gene encoded by C-5 sterol desaturase enzyme which introduces a double bond into the sterol ring structure can cause loss of function

of the enzyme and result accumulation of toxic sterols. This loss of function enables the *Candida spp.* to survive in the presence of azoles(Morio et al., 2012).

Zinc cluster member transcription factor family known as Sterol Uptake Control Protein 2 (Upc2) is an essential regulator of ergosterol metabolism that regulates the expression of the azole target gene ERG11. Upc2p is self-regulatory and is activated by azoles, low ergosterol levels, and anaerobic growth. Upc2p has an activation/regulatory domain at its C-terminus and a Deoxyribonucleic acid (DNA) binding domain at its N-terminus. Ergosterol negatively controls the transcription of UPC2 via attaching to the C-terminus of Upc2p. (Bhattacharya et al., 2020; Silver et al., 2004; Yang et al., 2015)

b) Other important mechanisms:

Increased multidrug efflux pumps expression, resulting in increased azole drug efflux from the fungal cell wall. Numerous efflux pumps, notably Cdr1p and Cdr2p from the ABC-Transporter superfamily and Mdr1p from the MFS-Transporter superfamily, are typically overexpressed in azole-resistant *C. albicans* strains. The overexpression in question is frequently caused by mutations in particular genes, like TAC1 and MRR1. As transcriptional activators of CDR genes, TAC1 mutations cause Cdr1p and Cdr2p to be upregulated. Similar to MRR1, Mdr1p is overexpressed as a result of MRR1 mutations (Escribano & Guinea, 2022; Franconi et al., 2023). Also, in fungi genomic plasticity which are aneuploidy and loss of heterozygosity (LOH) may be related with the azole resistance(Bhattacharya et al., 2020).

1.6.1 Primary mechanism for azole resistance related with the ergosterol biosynthesis pathway.

The ergosterol biosynthesis pathway is a crucial and complex series of biochemical reactions for fungal cell membrane integrity and function in *Candida* species. The pathway encompasses multiple enzymatic steps, each playing a pivotal role. The mevalonate pathway, which starts with acetyl-CoA and proceeds through a number of enzymatic transformations to produce squalene epoxidase, is one of the main pathways

involved. One essential step in the biosynthesis of ergosterol is production of lanosterol, which is produced by squalene epoxidase. To produce ergosterol, lanosterol passes through a series of demethylation processes, which is mainly facilitated by lanosterol demethylase (Erg11)(Dupont et al., 2012).

For the development of effective antifungal medications, it is important to understanding and strategic targeting of this ergosterol biosynthesis pathway.

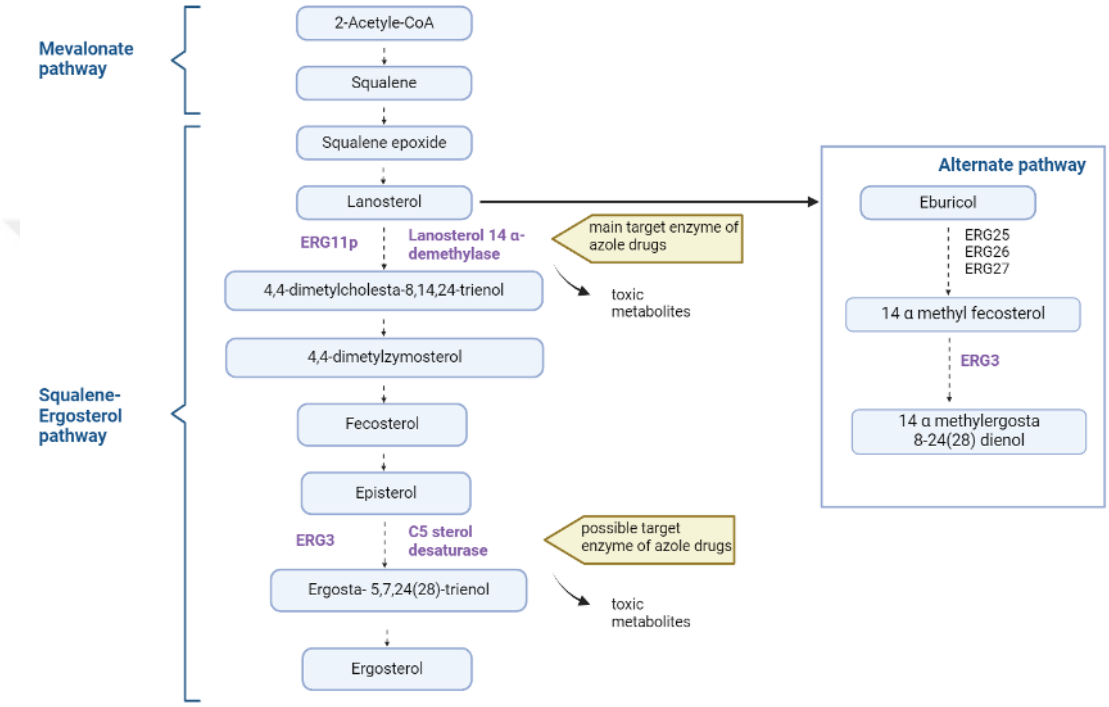

Figure 1.3: Ergosterol biosynthesis pathway (Bhattacharya et al., 2020)

1.6.2 Erg11 mutations and expressions related azole resistance

Human cells primarily constituted of cholesterol and the use of azoles does not interfere with human body cells during therapy because of differences between the membranes of fungal and human cells. Azole drugs suppress the synthesis of ergosterol, the main sterol of the fungal cell membrane. Triazole antifungal drugs suppress the ergosterol biosynthesis by attaching to the heme group in the target protein via a nitrogen group in their five-membered azole ring. This prevents the demethylation of C-14 of lanosterol, which causes methylated sterols to replace lanosterol in the membrane. When this enzyme is inhibited, toxic methylation intermediates accumulate and the amount of membrane ergosterol is depleted (Costa-de-Oliveira & Rodrigues, 2020). This causes

disruption of the fungal cell membrane function, growth inhibition, and occasionally even cell death. In the fungal cell membrane, ergosterol regulates the fluidity, permeability, and integrity of the membrane, similar to cholesterol in mammals. Azoles bind to lanosterol demethylase (14 α-demethylase), one of the key enzymes of ergosterol synthesis in the fungal cell, and irreversibly inhibit the enzyme. As a result of this suppression, toxic metabolites (14α-methyl sterol) accumulate inside the cell and the amount of ergosterol decreases, as a result of which the configuration of the fungal cell membrane changes (Figure *1.3*)(Akins, 2005; Escribano & Guinea, 2022).

Azole antifungal drugs, such as fluconazole, itraconazole, or voriconazole target and inhibit the specific enzyme lanosterol 14-α demethylase in the ergosterol biosynthetic pathway. Demethylation of the lanosterol is performed by this enzyme, inhibition of this enzyme results suppression of ergosterol synthesis and accumulation of toxic methylated sterols which impairs membrane functions (Dominique Sanglard et al., 2003).

The primary mechanism that causes azole resistance in *C. parapsilosis* is point mutations in the active region of the ERG11 gene, which encodes lanosterol demethylase, the target enzyme of ergosterol synthesis. The most common mutation detected in the ERG11 gene region is Y132F mutation, and this mutation is frequently encountered in fluconazole-resistant *C.parapsilosis* isolates (Demirci-Duarte et al., 2021). Y132F mutation detected in ERG11 has been found especially in association with epidemics, and it has been reported that isolates carrying this mutation have a high tendency to spread clonally(Corzo-Leon et al., 2021; Fekkar et al., 2021). Apart from this mutation, there are also ERG11p mutations in *C.parapsilosis* listed in the literature such as K143R, G458S, K128N, D133Y, D247G, G89V, I302T, L109F, M178T, N283Y, P406Q. Y132F mutation together with K143R,D421N,G307A and R398I are also found in other studies. moreover G548S the substitution may present with the Q250K and T519A substitutions (Choi et al., 2018; Escribano & Guinea, 2022). Apart from these mutations, some silent mutations in the ERG11 gene have been detected in both resistant and susceptible isolates, and the relationship of this polymorphism with resistance has not been clarified yet (Xu et al., 2008).

The lanosterol demethylase enzyme plays a key role in the synthesis of ergosterol, and the intermediate metabolites formed by the inactivation of this enzyme cause a toxic effect on the cell, leading to the death of the fungus with a fungistatic effect. They inhibit lanosterol demethylase enzyme competitively with azole group drugs. *Candida*, on the other hand, try to overcome this inhibition by increasing the amount of lanosterol

demethylase enzyme (Bhattacharya et al., 2020). Studies have shown that in addition to point mutations in ERG11 in *Candida*, a 2-fold increase in ERG11 gene mRNA level of Y132F positive isolates was found(Berkow et al., 2015). In another study, it was found that ERG11 mRNA expression was 1.5 to 7.4 times higher in fluconazole-resistant *C.parapsilosis* isolates containing the point mutation(Souza et al., 2015). In addition, Silva et al. observed an increase in ERG11 mRNA expression of azole-resistant *C.parapsilosis* isolates, but they found an increase in transcription factors related to ergosterol biosynthesis after exposure to azole drugs(Silva et al., 2011).

1.6.3 ERG3 and UPC2 related azole resistance mechanisms

Two most significant genes in the ergosterol biosynthesis pathway is ERG3 and ERG11, they play a key role in azole drug resistance(Zhou et al., 2018). When the function of 14-α demethylase is inhibited, causing the depletion of ergosterol production, ERG3 plays an important role. ERG3 is encoding an enzyme which is C-5 sterol desaturase responsible for converting nontoxic 14α-methylated sterol intermediates into the toxic sterol 14α-methyl-ergosta-8,24(28)-dien-3,6-diol. Inactivation or loss of this enzyme can cause increase in nontoxic ergosta-7,22-dienol. High levels of azole drug class resistance result from this interaction(Rybak et al., 2017).

According to previous studies in the literature, mutations in ERG3 have been shown to be associated with azole resistance in *Candida* species (Branco et al., 2023; Morio et al., 2012). This enzyme catalyzes one of the last steps in the synthesis of ergosterol, and under azole treatment, non-toxic intermediate products can accumulate, potentially altering the fungal cell membrane's composition. Therefore, with mutations in the ERG3 gene, the fungus inactivates or transforms the enzyme, thus gaining resistance to azole drugs. Studies conducted in *C. albicans* isolates have shown a negative correlation between ERG3 expression level and azole sensitivity (Feng et al., 2019). On the other hand, Branco et al. reported in their study that homozygous “missense point mutations” in the ERG3 gene in *C.parapsilosis* isolates, R135I mutation causes an increase in the expression of the ERG3 gene and prevents the formation of toxic intermediate metabolites. As a result, point mutations in the ERG3 gene and the relationship between mRNA expression level and azole resistance has not yet been clarified (Branco et al., 2017).

Since ergosterol is an essential sterol of the fungal cell membrane, the amount of enzymes encoding ergosterol synthesis in the cell is kept under control by various regulatory factors. One of the most important molecules known to control the expression of enzymes involved in sterol synthesis is UPC2, the zinc group transcription activator. It has been shown that gain-of-function mutations in the gene encoding this molecule cause azole resistance by increasing the expression of genes encoding sterol synthesis enzymes(Flowers et al., 2012). In another study, it was shown that deletions in the UPC2 gene in candida cause an increase in azole sensitivity, and it was proposed as a new drug target site for azole drugs (Gallo-Ebert et al., 2014).

A key transcriptional regulator, UPC2 is essential to the pathway leading to ergosterol production in *Candida* species. The zinc cluster transcription factor Upc2, which is activated in response to ergosterol deprivation, is responsible for controlling the expression of ERG genes, including ERG11 which codes for the essential enzyme lanosterol 14-α-demethylase. Research indicates that the overexpression of UPC2 causes a rise in ERG11 transcription, which in turn raises the levels of Erg11p. By increasing ergosterol production, this overexpression may mitigate the inhibitory effects of azoles on Erg11p. ERG11 overexpression and increased fluconazole resistance are frequently caused by gain-of-function mutations in Upc2, which result in the upregulation of target genes. However, not every instance of ERG11 overexpression is associated with UPC2 mutations(MacPherson et al., 2005; Morschhäuser, 2016; White & Silver, 2005).

1.7 Azole resistance related metabolomic changes in Candida species

The most important effect of azole drugs is to suppress the target enzyme and to ensure the formation of toxic intermediates in the cell. The effect of these toxic intermediates on the metabolic pathways of the fungal cell is not yet fully known. Biological synthesis and degradation pathways in eukaryotic fungal cells are controlled by many intermediate molecules. There are a very limited number of studies showing the effects of the strategies developed by the cell to survive against the accumulation of toxic metabolites on these pathways and end products. As the methods used to create metabolomic profiles have progressed, new studies have started in this field as well, and researchers have conducted metabolomic studies in different fungi with different analysis techniques. Metabolomics research is a systematic biology approach that aims to show

the presence and density of all small molecular weight metabolites in a biological sample, rather than examining a single metabolite. Metabolomic approaches stand out as an important technique, especially in the discovery of new biomarkers. For this purpose, methods such as high-performance liquid chromatography mass spectrometry (HPLC-MS) and gas chromatography-mass spectrometry (GC-MS) were used in studies with yeasts (Madji Hounoum et al., 2015).

Katragkou and friends are investigated the effects of fluconazole on the metabolomic profile of the *C. albicans*. The researchers treated susceptible *C.albicans* isolate which Minimum Inhibitory Concentration (MIC) value was 4 mg/L with different concentration of fluconazole (0.25 MIC, 0.5 MIC, 1 MIC) and intracellular metabolites were extracted and examined by LC/MS-based metabolomic profiling. 64 metabolites have been identified and of those abundance of 12 metabolites has changed under the fluconazole exposure. The main findings include elevated concentrations of mevalonate and the intermediates of central carbon metabolism (a-ketoglutarate, glucose-6-phosphate, phenylpyruvate, and ribose-5-phosphate). Furthermore, there was a decrease in the amount of guanine and five amino acids (glycine, proline, tryptophan, aminoisobutanoate, and asparagine) in response to fluconazole (Katragkou et al., 2016). To our knowledge, up to date, there is no exiting study that is focusing on the metabolomic changes in fluconazole resistant *C.parapsilosis* isolates under drug pressure.

It is critical for the early identification of resistance and the proper initiation of antifungal treatment that resistant isolates exhibit cellular alterations resulting from resistance. Our aim in this study is to demonstrate point mutations in the ERG11 gene, which encodes lanosterol demethylase, the target enzyme of fluconazole, and the ERG3 gene, which encodes C-5 sterol desaturase, one of the possible targets, in fluconazole-resistant *C. parapsilosis* isolates, and to examine the changes in the expression of these genes (ERG11, EEG3 and UPC2) at the mRNA level. Additionally this study will reveal the changes of intracellular metabolites of *C. parapsilosis* isolates which have different mutations under the fluconazole exposure (0 MIC, 0.5 MIC, 1 MIC) by NMR spectroscopy method.

Chapter 2:
METHODOLOGY

2.1 Selection of isolates, Culture media and Growth Conditions

In this study, 15 fluconazole non-susceptible *C. parapsilosis* isolates obtained from blood cultures of patients diagnosed with candidemia from three different tertiary university or state hospitals between 2016 and 2018 were included. Species-level identifications of *C. parapsilosis* isolates were confirmed by matrix-assisted laser desorption ionization-time-of-flight mass spectrometry (MALDI-TOF MS) in the clinical microbiology laboratory of Koc University Hospital. These isolates were sent to Koç University Faculty of Medicine, Koc University-Is Bank Center for Infectious Diseases (KUISCID) mycology laboratory and stored at (-80 °C) for further analysis. *C. parapsilosis* ATCC 22019 and *C.krusei* ATCC 6258 were used as reference strains in this study.

2.2 Antifungal Susceptibility Tests

The antifungal susceptibility tests of all previously reported as fluconazole non-susceptible isolated were repeated for confirmation in this thesis study. Antifungal susceptibility tests were performed by broth microdilution method according to CLSI references at Koc University Faculty of Medicine, KUISCID, Mycology Research Laboratory (Istanbul, Turkey). The interpretation of susceptibility test was performed according CLSI methodology, as well (CLSI, 2013; Pfaller & Diekema, 2012).

2.2.1 Medium preparation

RPMI 1640 (with glutamine, without bicarbonate, and with phenol red as pH indicator) has been used for susceptibility tests. The formula of the RPMI 1640 medium buffered with 0.165mol/L MOPS is provided in the table below Table *2.1*. Powdered medium is dissolved in 900 ml H_2O and MOPS is added, then pH is adjusted to 7.0 with 1 M sodium hydroxide, final volume arranged to 1 L. Sterilized by using a 0.22 um pore-sized filter and stored 4 ℃ (RPMI medium D-glucose rate is 0.2%).

Table 2.1:RPMI 1640 (with glutamine, without bicarbonate, and with phenol red as pH indicator) compositions

Ingredient	**Amount(g)**
Powder RPMI 1640 medium (with glutamine and phenol red, without bicarbonate)	10.4
MOPS (3-[N-morpholine] propane sulfonic acid) buffer	34.53

2.2.2 Preparation of stocks of antifungal agents

In this study, fluconazole (Sigma Aldrich, USA), voriconazole (Sigma Aldrich, USA) and posaconazole (Sigma Aldrich, USA) antifungals were used. Stock solutions are prepared according to the below formula;

$$\text{Weight(mg)} = \frac{Volume\ (ml) x\ Concentration\ (\frac{ug}{ml})}{Assay\ potency\ (\frac{ug}{mg})}$$

Antifungal agents are diluted in a liquid growth medium (RPMI-1640) to provide a variety of concentrations. These concentrations range throughout a two-fold dilution series that begins at a higher concentration and gradually decreases. Two-fold serially diluted 50 µl medium is plated to 96 well which range from 64 µg/ml to 0.125 µg/ml for fluconazole and range from 16 ug/ml to 0.313 ug/ml for posaconazole and voriconazole.

2.2.3 Preparation of fungal inoculum

C. parapsilosis isolates, obtained from clinical culture collections grown on Sabouraud dextrose agar by incubating at 37 ℃ temperature. After obtaining a pure culture from 48 h *C. parapsilosis*, suspension of fungal cells is prepared in a sterile Phosphate Buffer Saline (PBS) solution. A specific turbidity standard (0.5 McFarland) is used to determine the density of the suspension. This 0.5 McFarland standard is equivalent to 1–5 × 10^6 colony-forming units per milliliter (CFU/mL). A working suspension is arranged to 1–5 × 10^3 CFU per ml by diluting the 0.5 McFarland followed by 1:20 and 1:50 dilution with RPMI 1640 medium.

2.2.4 Inoculation of microdilution plates

Each well of the microdilution plate filled with 50 µl standardized 1:50 and 1:20 diluted 0.5 McFarland fungal inoculum (1x10^3 to 5x10^3) and 50 µl RPMI medium, so inoculum is diluted 1:1 and when the cells inoculated desired final inoculum size is achieved. (with

the final inoculum $0.5x10^3$ to $2.5x10^3$ cells per ml).The plate was then incubated in a specific period (24 h and 48 h), at 35-37 ℃ temperature which is the optimum temperature for fungal growth.

2.2.5 Interpretation of results

Minimum inhibitory concentrations (MIC) were assessed visually after 24 and 48 hours if available using species-specific CLSI clinical breakpoints ("Clinical Breakpoints-CBP") given in Table *2.2* and if don't have CBP they were assessed according to epidemiological cut-off values ("Epidemiological Cut-off Values - ECV") for *C. parapsilosis* given in Table Z (CLSI, 2013; Pfaller & Diekema, 2012). *C. parapsilosis* ATCC 22019 and *Candida krusei* ATCC 6258 strains are used as reference control strains in all experiments of the study. All intermediate and resistant results were accepted as non-susceptible for this study.

Table 2.2:Interpretive Guidelines for In Vitro Susceptibility Tests for *Candida parapsilosis*

Antifungal Agent	**Species**	**MIC Range (µg/ml)**				
		CBP			**ECV**	
		S Susceptible	**I Intermediate**	**R Resistant**	**WT**	**Non-WT**
Fluconazole	*Candida parapsilosis*	≤2	4	≥8	≤2	>2
Voriconazole		≤0.12	0.25-0.5	≥1	≤0.12	>0.12
Posaconazole		NA	NA	NA	≤0.25	>0.25

2.3 Sanger Sequence

In this study, analysis of the point mutations in the ERG11 and ERG3 genes of *C. parapsilosis* is performed by Sanger sequencing for all fluconazole non-susceptible isolates. The Sanger sequencing method is described below.

2.3.1 DNA Isolation

For DNA isolation, in the first step; 95 µl nuclease free (NF) water, 95 µl solid tissue buffer (Zymo Quick DNA Miniprep Plus Kit, Catalog Number: D4068,), and 50 µl 2500

U/ml (125 U) Lyticase (Sigma-Aldrich, Merck Group, Germany) total 240 µl mixture is prepared in an eppendorf tube and one loopful of *C. parapsilosis* colonies are added into the mixture and gently pipetted without vortexing. After incubation at 37 ℃ for onehour, the mixture is centrifuged at 10,000 g for one minute 30 seconds at room temperature. The supernatant was removed and 95 µl Nuclease Free (NF) water, 95 µl solid tissue buffer, and 10 µl Proteinase K were onto the cell pellet, this cell mixture was incubated at 55 ℃ for one hour. Then, centrifuged at 10,000 g for one minute 30 seconds at room temperature. DNA isolation from pellets applied with commercial DNeasy Ultraclean Microbial Kit (QIAGEN, USA) according to manufacturer's instructions with slight modifications. Extra washing steps are added to the procedure. From 50 µl elution, the sample quality was assessed through DNA concentration and the 260/280 and 260/230 ratios using a Nanodrop spectrophotometer (Thermo Scientific™, USA). Acceptable range for A260/230 is 2.0-2.2 and for 260/280 is ~1.8. The purified DNA serves as the template for sequencing.

2.3.2 Polymerase Chain Reaction (PCR)DNA Amplification (Conventional PCR)

Table 2.3:List of the primers used for Sanger Sequence experiments.

Oligonucleotide	**Sequence (5' → 3')**	**Purpose**	**References**
ERG11_F1	CGAGATAATCATCAACGAACATTC	ERG11 Sanger Sequence	(Souza et al., 2015)
ERG11_R1	CGTTTAAAACATCCAAAGACCTTA		
ERG11_F2	AAAGACCGCATTGACTACCGAT		
ERG11_R2	AATCTGAGGGTTTCCTTGATGGT		
ERG3_F	CCCACGTTTATTTCACTAGATCC	ERG3 Sanger Sequence	(Berkow et al., 2015)
ERG3_R	GTGTCCCTATTGCCCATTCCC		

DNA amplification reactions were performed with the 12.5 µl commercial DreamTaq Green PCR master mix, 0.5 µl 25 pmol forward and reverse primers (Table *2.3*),0.5 µl DNA of the isolates, and nuclease-free water is added to make the total PCR volume to 25 µl. The following reaction conditions were used; initial denaturation at 94°C, two min., 40 cycles of denaturation at 94°C, 15 sec., annealing at 60 C, 30 sec., extension at 72°C, 20 sec. and lastly final extension at 72°C, 5 min. Amplicons were run on 1.5 % agarose gel stained with Ethidium Bromide.

2.3.3 PCR Clean up, Sequencing Reaction & Electrophoresis

Amplified products were purified with the NucleoSpin Gel and PCR Clean-up kit (Macherey-Nagel, Germany) according to the manufacturer's instructions. Firstly, 25 µl reaction mixtures were adjusted to 50 µl with nuclease-free water and mixed with 100 µl NT1 Buffer. Mixtures were loaded into NucleoSpin Gel and PCR Clean-up Column and centrifuged at 11.000 g for 30 seconds. 700 µl Buffer NT3 was added to the column and centrifuged for 30 seconds at 11,000 x g. Flow-through is discarded and columns are centrifuged for one minute at 11.000 g for silica membrane drying. The cleaned PCR product is eluted with 20 µl NE buffer from the membrane.

The BigDye Terminator v3.1 Cycle (Applied Biosystems, U.S.), which amplifies products based on the dideoxy-chain termination technique, was used to amplify the purified products. The given protocol was used to amplify the products; two µl BigDye, one µl BigDye buffer, three twenty µl one pmol primer, and one µl purified PCR product were added and the total volume was arranged to 20 µl. PCR conditions were one minute at 96°C followed by 25 cycles of 10 seconds at 96°C, five seconds at 50°C, and finally four minutes at 60°C. The resulting products were purified with the ZR-96 DNA Sequencing Clean-up Kit (Zymo Research, U.S.). 240 µl sequencing binding buffer is added to the sequencing reaction and centrifuged at 2576 g for three minutes. For the washing step, 300 µl sequencing wash buffer is added to each well and centrifuged at 2576 g for seven minutes. The sequencing reaction products are sequenced by using Applied Biosystems ABI 3500 Genetic Analyzer.

2.3.4 Sequence Analysis

Base calling and trimming of electropherograms (*.ab1 files) obtained from the ABI 3500 genetic analyzer (Applied Biosystems, United States) were performed with the KB BaseCall algorithm using the Sequencing Analysis software, and bi-directional readings were obtained. The sequences GQ302972.1 for the ERG11 gene and KT277771.1 for the ERG3 were used as references and the alignment and editions were performed using the SeqMan (Version 5.0) program. Thus, a common (consensus) sequence for each sample was created. Collective assembly, alignment and mapping of the generated sequences were performed with the ClustalW package included in the BioEdit (Version 7.2.5) Program. Base mutation coordinates were determined from these sequences after

mapping, and their possible effects were reported by converting them to amino acid data with the translation module included in the BioEdit (Version 7.2.5) program.

2.4 Growth curve analysis and cell collection for mRNA expression and metabolomic studies

To examine the growth kinetic of fluconazole resistant *C. parapsilosis* isolates, firstly, the growth curves of *C. Parapsilosis* ATCC 22019 strain were calculated, and the midpoint of the exponential growth phase was determined. For mRNA expression and Nucleic Magnetic Resonance Spectroscopy (NMR) analyses, the midpoint of the exponential phase of yeasts was determined as the standard time interval in which all measurements were made at this specific point. For this purpose, each of the isolates containing five ml of *C.parapsilosis* suspension adjusted as 0.5 McFarland was placed in flasks containing 40 ml of RPMI medium containing 2% glucose. Afterwards, five ml of sterile distilled water was added to give a total volume of 50 ml in each bottle. The bottles were incubated at 35 °C at 135 rpm in a constantly shaking oven, and the midpoint of the exponential phase was determined by measuring the optical density (OD) at 550 nm at one-hour intervals (Nordin et al., 2013). When OD550 nm reached 0.8-1.0, cells were extracted for mRNA expression experiments and metabolomic studies.

All genomic experiments were performed on fluconazole non-susceptible isolates without exposing the isolates to fluconazole. In selected isolates (according to their resistance mechanisms and point mutations) whose resistance genes are revealed, mRNA expression experiments and metabolomic experiments were performed at 0.5 MIC, 1 MIC under fluconazole, and the change of metabolites and transcripts were monitored according to fluconazole drug exposure.

2.5 Quantitative Real-Time Polymerase Chain Reaction (qRT-PCR)

In selected isolates according to their mutations in ERG11 and ERG3 genes, mRNA expression experiments were performed at 0.5 MIC, 1 MIC under fluconazole drug exposure. The growth curve of the isolates was monitored, when Optical Density (OD)550 nm reached 0.8-1.0, cells were extracted for mRNA expression experiments.

The mRNA expression levels of and ERG11 gene encode the azoles target enzyme lanosterol demethylase (14 α-demethylase), and the ERG3 gene encodes possible target enzyme C-5 sterol desaturase and transcription factor UPC2 gene (general transcriptional

activator in Candida species) in *C. parapsilosis* were determined by qRT-PCR assay with specific primers (Table *2.4*). The cycle threshold point CT values were normalized according to the internal control actin (ACT1) gene. (CT) value, which is the cycle number at which a PCR product can be identified above the fluorescent background signal, was used to calculate the mRNA expression levels of the ERG11, ERG3 and UPC2 genes. CT values were calculated for each target gene ERG11, ERG3, UPC2 genes and housekeeping (β-actin) gene. For calculation of relative quantification of mRNA expression ΔΔCT algorithm was used. Using actin as a housekeeping gene, fold changes in gene expression were determined using the $2^{\Delta\Delta CT}$ method. *C.parapsilosis* ATCC is used to normalize the expression levels, specificity of the products were checked with melting curves.

Table 2.4: List of the primers used for RT-PCR experiments.

Oligonucleotide	**Sequence (5' → 3')**	**Purpose**	**References**
qERG11_F	GTACACCGTCATTACTCTACCCAACA	ERG11 Real time PCR	(Souza et al., 2015)
qERG11_R	TGCTCCTTTCATTTACAACATCATTT		
qERG3_F1	ATGCTTTCCACCCAGTTGAT	ERG3 Real time PCR	(Branco et al., 2017)
qERG3_R1	ACTACAGGGTCATTGCTCAT		
qUPC2-F1	ATTGGAGTGTGGGTATCTTCAT	UPC2 Real time PCR	(Silva et al., 2011)
qUPC2-R1	CCTTCGCCTTCTTCAGTTC		
ACT	ATGATAGAGTTGAAAGTAGTTTGGTCAATA	ACTIN Real time PCR	(Rossignol et al., 2007)
ACT	ACTACTGCTGAAAGAGAAATTGTTAGAGAC		

2.5.1 RNA Isolation

C. parapsilosis cells were grown in 50 ml RPMI liquid medium until their mid-log phase, when OD550 nm reached around 0.8 to 1, cells were harvested to falcon tube and centrifuged 5.000 g, 5 min at room temperature. For RNA isolation Trizol based method was used with some modifications (Roth et al., 2018). For this purpose, yeast pellets were immediately frozen with liquid nitrogen and 1 ml Trizol (Invitrogen, US) put into cell pellet with QIAGEN DNeasy silica beads, vortexed with a max speed of 15 min. The samples were centrifuged at 13000 rpm for 15 min at 4°C to remove extracellular material

and silica beads. Transferred supernatant mixed with 0.2 ml chloroform vigorously shaken by hand for 15 seconds and incubated for three min at room temperature. Samples were centrifuged at 13000 rpm for 15 minutes at 4°C for phase separation, upper aqueous phase which includes RNA precipitated with 0.5 ml isopropanol by incubating 10 minutes in room temperature. Centrifuged at 13000 rpm for 10min at 4°C to obtain pellets and pellets were washed with %75 ice-cold ethanol. Centrifuged at 10.000 g for 5 minutes at 4°C. The remaining %75 ethanol at the bottom is dried by waiting approximately 15-30 minutes. When the pellet is dried, 50 µl nuclease-free water is used for resuspension of the pellet by pipetting gently and incubating in 60 °C water bath. RNA quality and concentrations were measured with a Nanodrop 2000 Spectrophotometer (Thermo Scientific, US).

2.5.2 Complementary DNA (cDNA) Synthesis

For cDNA synthesis, the Biorad iScript™ cDNA Synthesis Kit (Biorad, USA, cat. number: 1708891) was used according to manufacturer instructions. four µl 5x iScript reaction mix, one µl, iScript reverse transcriptase, RNA template and nuclease-free water mixture 15 µl was used for PCR reaction that performed with Veriti 96-Well Thermal Cycler (Thermofisher, USA) apparatus. PCR was performed according to the following reaction: priming at 25°C for five minute, followed by reverse transcription step at 46°C for 20 min, then RT inactivation at 95°C for one minute. After the cDNA synthesis reaction concentrations were arranged by nuclease-free water to reach 200 ng cDNA/µl for each qRT-PCR analysis well.

2.5.3 Quantitative Real-Time Polymerase Chain Reaction

Quantitative real-time PCR (qRT-PCR) was performed by using the QuantStudio™ 3 Real Time PCR instrument (Thermo Scientific, USA). Analysis of mRNA expressions of the respective genes of *C. parapsilosis* isolates were performed with PowerUp SYBR Green Master Mix (Thermo Scientific, USA- Catalog no: A25742). Each well received a total of 20 µl of mixture, which included 10 µl of SYBR Green I Master, 10 µl of forward and reverse primers at a working concentration of 10 µM, 50 ng of cDNA, and nuclease-free water. Thermal cycling conditions: it was performed as an initial step for five minutes at 95°C, followed by a 15 seconds denaturation at 95°C, a 25 seconds primer attachment at 60°C, and a 30 seconds extension at 72°C for a total of forty cycles. Then, a melting

curve was followed by heating from 60°C to 95°C with a temperature unit difference of 1.6°C. qRT-PCR experiments were performed by running in triplicate for all samples and genes.

2.6 Nuclear Magnetic Resonance Spectroscopy (NMR)

2.6.1 Metabolite extraction procedure for NMR

Each of the chosen isolate for metabolomic analysis was grown as three separate flasks until their growth curve reached the midpoint of the exponential phase and centrifuged at 4500 rpm for 30 minutes. The cell pellet was washed 2 times with cold water and directly on the pellet 5 mL of 75% ethanol v/v solution at 80°C was poured with DNeasy Ultraclean Microbial Kit silica beads and vortexed for 30 seconds two times, heated to 80°C for three minutes, and again two times 30 seconds vortexed. After removing the supernatant, the beads were washed with another 2 mL of 75% ethanol v/v, the combined extract was centrifuged (10 min, 16,000 g) to remove cell debris and then the supernatant was taken and lyophilized at 30°C in a rotary vacuum concentrator (Eppendorf, UK/Ireland).

Extracted and lyophilized intracellular metabolites were dissolved in D2O buffer containing 37.7 mM Na2HPO4, 12.3 mM KH2PO4, and 20 mM NaCl, with a pH value of 7.4. 1 mM DSS was added to the buffer solution as an internal marker. Then, the solution containing the metabolites were placed in a 5 mm NMR tube (Hilgenberg GmbH, Germany) and placed in a 500 MHz Bruker NMR spectrometer for analysis.

One-dimensional 1H-NMR spectra were performed using a 5 mm BBO RT probe on the Bruker Avance Neo 500 MHz NMR spectrometer located in the infrastructure of Koç University Nano-fabrication and Nano-characterization Application and Research Center for Scientific and Technological Advanced Research (n2STAR).

2.6.2 NMR statistical analysis

NMR data divided into 0.02 ppm-sized data packets. Datasets coded as (Bin.x.xx [ppm]) to hold the information. Examination of the datasets were performed by using MetaboAnalyst 5.0 statistical analysis tool. Different normalization techniques are used for discrimination of the groups. And, better technique for the discrimination has been decided, then all data points normalized according to square root transformation-auto

scaling normalization technique. Partial Least-Squares Discriminant Analysis (PLS-DA) is a classification and discrimination technique based on the Partial Least Squares (PLS) regression approach. To identify differences between classes, this method is commonly applied, especially in high-dimensional and multivariate datasets. PLS-DA is a widely used technique for the analysis of biological systems that are complicated, such metabolomic research.

The PLS-DA results were assessed using a graph known as the Variable importance in projection (VIP) projection variable significance score graph. The VIP scores, which evaluate each variable's (such as metabolites) significance in the categorization, identified the most crucial elements. VIP scores were calculated based on each variable's contribution to the PLS-DA model's components (latent variables). Elevated VIP scores, starting at 1, indicate that the variable holds greater significance in terms of classification. Although this cutoff number may vary in practice, important variables typically have VIP ratings greater than 1. This graphic makes it easy to identify important elements visually and focus the study on those that need to prioritize. Subsequently, we identified the metabolites of the peaks in the relevant ppm values that comprise the data packages (Bin.x.xx) in the VIP score graph by closer inspection. For this technique, the NMR spectra were reopened, and the metabolites associated with the peak in the appropriate ppm area were determined using Chenomx software.

Flow chart of methodology of this study is given below Figure 2.1.

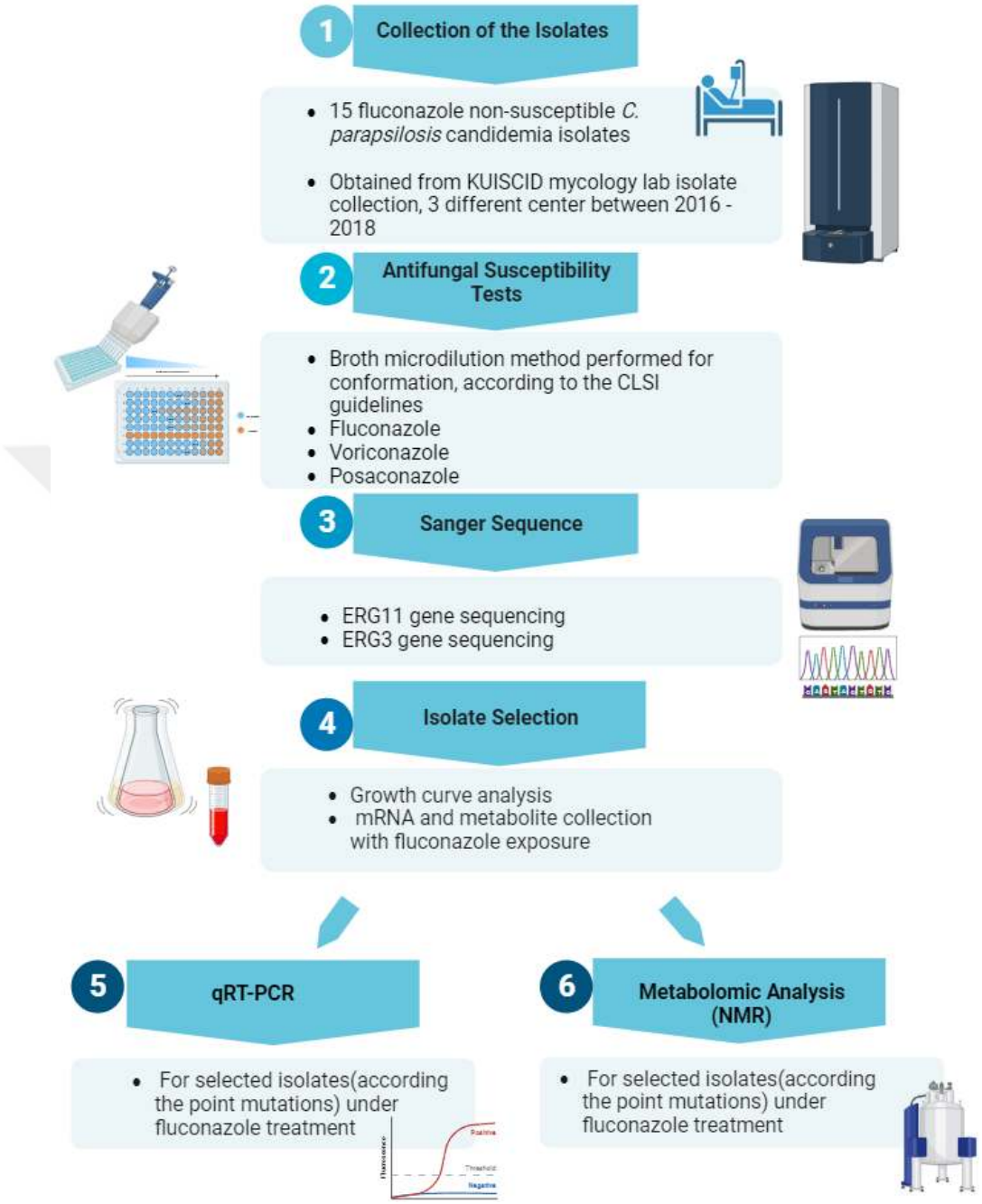

Figure 2.1: Flow chart of the study

2.7 Ethical Statement of the Study

The ethical Statement of this study is given by the Koç University Committee on Human Research with the number 2023.176.IRB2.041.

Chapter 3:
RESULTS

3.1 Isolate Selection and Antifungal Susceptibility Tests Results

In this study, 15 fluconazole non-susceptible *C. parapsilosis* isolates obtained from blood cultures of patients diagnosed with candidemia from three different tertiary university or state hospitals between 2016 and 2018 were included (Table *3.1*).

Table 3.1:Isolates according to their isolation years and sources

Isolate Code	Hospital	Date
388	Koşuyolu High Specialty Training and Research Hospital, Istanbul Provincial Health Directorate	February,2016
406		February,2016
416		March,2016
420		April,2016
424		April,2016
456		July,2016
478		July,2016
481		August,2016
519		August,2016
548		August,2016
737		September,2017
814	Baskent University Hospital, Istanbul	June,2016
1186	Koc University Hospital, Istanbul	August,2018
1200	Koc University Hospital, Istanbul	April,2018
1207	Koc University Hospital, Istanbul	December,2018

The Minimum Inhibitory Concentration (MIC) values of the non-susceptible *C.parapsilosis* isolates were confirmed according to CLSI guidelines for fluconazole, voriconazole, and posaconazole antifungal drugs. MIC results were given in Table *3.2* and MIC_{50} and MIC_{90} results were given Table *3.2*.

All of the isolates were non-susceptible to fluconazole, 7/15 (47%) of the isolates were non-susceptible to voriconazole, 5/15 (33%) of the isolates were non-wild type for posaconazole. Clinical Breakpoints (CBP)s was not available for the posaconazole, therefore Epidemiologic cut-off values (ECV)s was used for the interpretation of the results. All voriconazole non susceptible isolates which is 33% of the total were also non-susceptible to fluconazole and voriconazole drugs. These 33% of the isolates were pan-azole resistant.

Table 3.2:Minimum Inhibitory Concentration (MIC) results of *C. parapsilosis* isolates

Isolate Code	FLU ug/ml	Result	VRC ug/ml	Result	PSC ug/ml	Result
416	**32**	**Resistant**	**0 .5**	**Intermediate**	**0 .5**	**non-WT**
456	**16**	**Resistant**	0 .06	Susceptible	0 .125	WT
737	**16**	**Resistant**	**0 .25**	**Intermediate**	**0 .5**	**non-WT**
388	**8**	**Resistant**	**0 .25**	**Intermediate**	**0 .5**	**non-WT**
406	**8**	**Resistant**	**0 .5**	**Intermediate**	0 .03	WT
420	**8**	**Resistant**	0 .125	Susceptible	0 .125	WT
424	**8**	**Resistant**	0 .125	Susceptible	0 .25	WT
481	**8**	**Resistant**	0 .125	Susceptible	0 .06	WT
1207	**8**	**Resistant**	0 .125	Susceptible	0 .25	WT
478	**4**	**Intermediate**	0 .03	Susceptible	0 .03	WT
519	**4**	**Intermediate**	0 .125	Susceptible	0 .03	WT
548	**4**	**Intermediate**	**0 .25**	**Intermediate**	0 .06	WT
814	**4**	**Intermediate**	**0 .5**	**Intermediate**	**0 .5**	**non-WT**
1186	**4**	**Intermediate**	**0 .25**	**Intermediate**	**0 .5**	**non-WT**
1200	**4**	**Intermediate**	0 .06	Susceptible	0 .125	WT

All non-susceptible isolates were indicated with bold type. WT: wild-type, non-WT: non-wild type
FLU: fluconazole, VRC: voriconazole, PSC: Posaconazole

Table 3.3:Fluconazole non-susceptible *C.parapsilosis* isolates MIC50 and MIC90 values

Antifungal	MIC (µg/mL)		
	MIC_{50}	**MIC_{90}**	**Range**
FLU	8	16	2 to 32
VRC	0.125	0.5	0.03 to 0.5
PSC	0.125	0.5	0.03 to 0.5

FLU: fluconazole, VRC: voriconazole, PSC: Posaconazole

3.2 Analysis of point mutations by Sanger sequencing

3.2.1 DNA isolation Results

For the analysis of the point mutations in ERG11 and ERG3 genes, the isolates firstly, DNAs were isolated as described in Section 2.3.1. The A260/230 values for extracted DNAs were ranged between 0.732-2.126.and the 260/280 values were detected as 1.725-1.875. The DNA concentrations were between 27 ng/µl to 166 ng/µl.

3.2.2 Sanger Sequence Results

ERG11 gene substitutions

According to Sanger sequence results, it has found that 10/15 (66%) of the isolates were harboring Y132F mutations in their ERG11 gene (Table 3.4). Adenine is changed to Thymine in 395th nucleotide sequence and this cause a change in Tyrosine amino acid to Phenylalanine amino acid (A395T → Y132F), shown in Figure *3.1*

Table 3.4:ERG11 gene Sanger sequence results

Number	Isolate Code	Mutation ERG11 gene	Homozigot/Heterozigot
1	388	None	None
2	406	Y132F	Homozigot
3	416	Y132F	Homozigot
4	420	Y132F	Homozigot
5	424	Y132F	Homozigot
6	456	Y132F	Homozigot
7	478	K143R+R398I	Homozigot/Homozigot
8	481	Y132F	Homozigot
9	519	Y132F	Homozigot
10	548	Y132F	Homozigot
11	737	None	None
12	814	None	None
13	1186	Y132F+R398I	Homozigot/Homozigot
14	1200	Y132F+R398I	Homozigot/Homozigot
15	1207	K143R	Homozigot

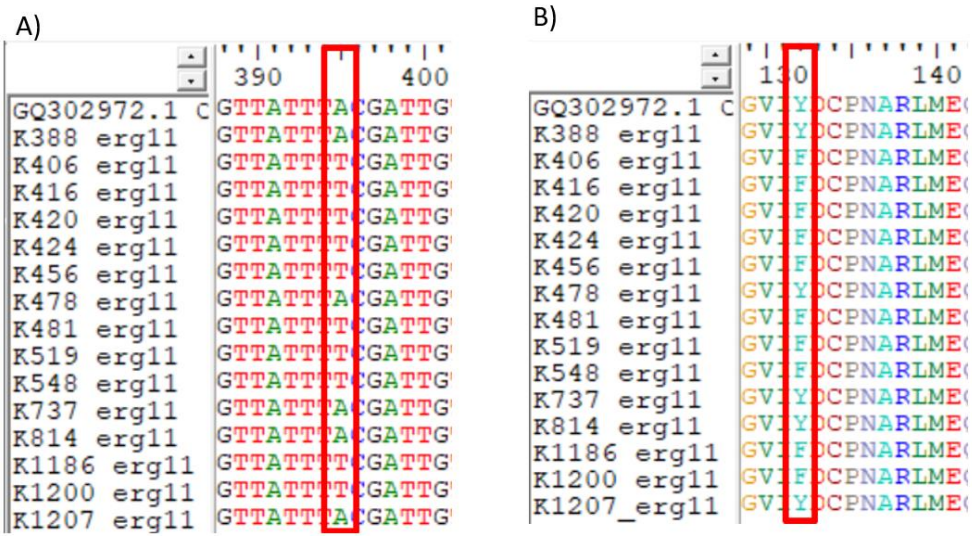

Figure 3.1: ERG11 gene Y132F substitution. A) nucleotide demonstration B) amino acid demonstration

Sanger sequence results indicate that besides the most common Y132F mutation in ERG11 gene, *Candida parapsilosis* isolates were carrying the K143R and R398I which are shown in the literature. When a Guanine to Adenine substitution occur in the 428th amino acid, it causes change of Lysine (K) amino acid to Arginine (R), (A428G→K143R)(Figure *3.2*)

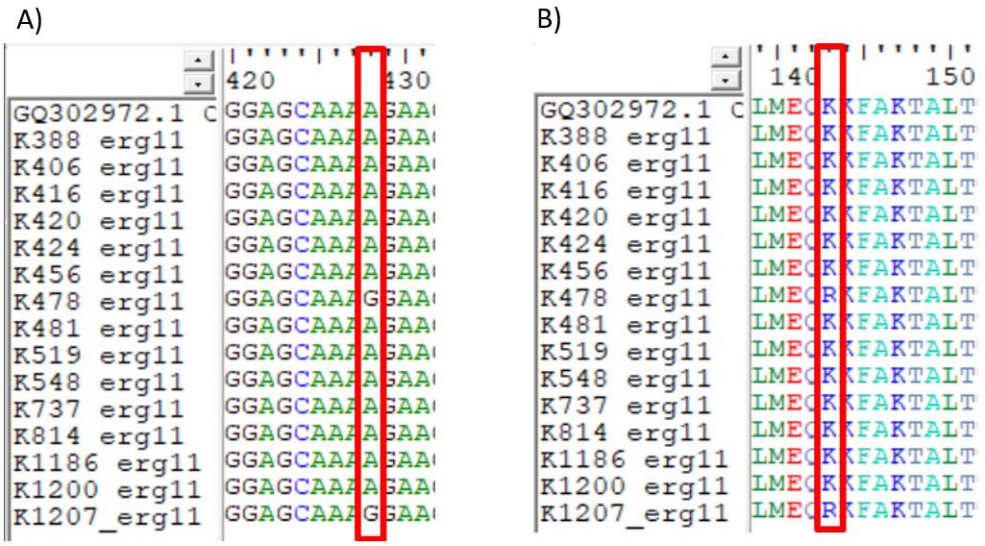

Figure 3.2: ERG11 gene K143R substitution A) nucleotide demonstration B) amino acid demonstration

Another mutation found in the sequenced isolates was R398I substitution. Guanine is changed to Thymine in 1193th nucleotide sequence and this cause a change in Arginine amino acid to Isoleucine amino acid (G1193T → R398I), shown in Figure 3.3.

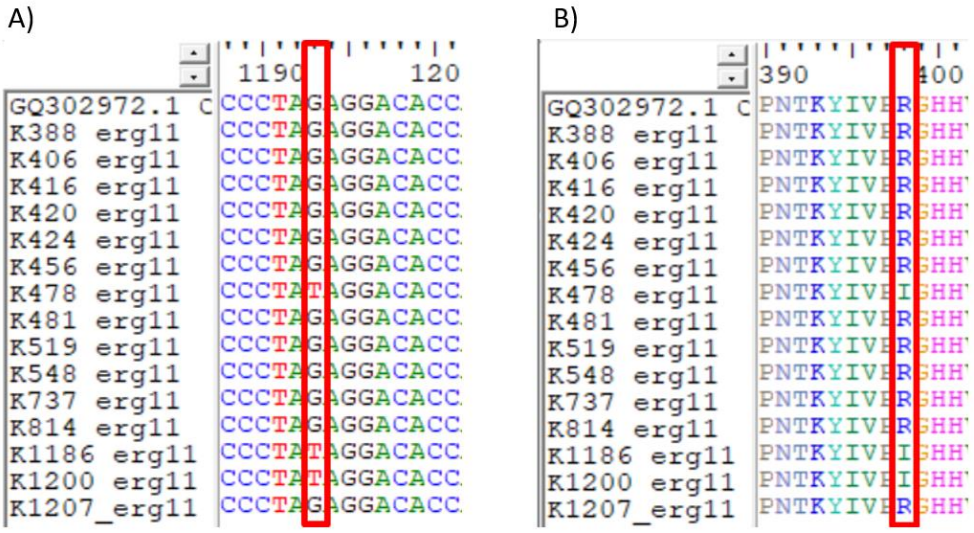

Figure 3.3:ERG11 gene R398I substitution A) nucleotide demonstration B) amino acid demonstration

ERG3 gene substitutions

ERG3 gene Sanger sequence results showed that 11 of the 15 isolates were carrying homozygote silent mutation (Table 3.5). Cytosine nucleotide changed to Thymine nucleotide however this point mutation does not disrupt to functioning of the protein. Histidine amino acid does not change when the mutation occurred(Figure *3.4*).

Table 3.5: ERG3 gene Sanger sequence results

Number	Isolate Code	Mutation ERG3 gene	Homozigot/Heterozigot
1	388	C825T (H275H)	Homozigot
2	406	C825T(H275H)	Homozigot
3	416	C825T(H275H)	Homozigot
4	420	C825T(H275H)	Homozigot
5	424	C825T(H275H)	Homozigot
6	456	C825T(H275H)	Homozigot
7	478	None	None
8	481	C825T(H275H)	Homozigot
9	519	C825T(H275H)	Homozigot
10	548	C825T(H275H)	Homozigot
11	737	C825T(H275H)	Homozigot
12	814	None	None
13	1186	None	None
14	1200	None	None
15	1207	C825T(H275H)	Homozigot

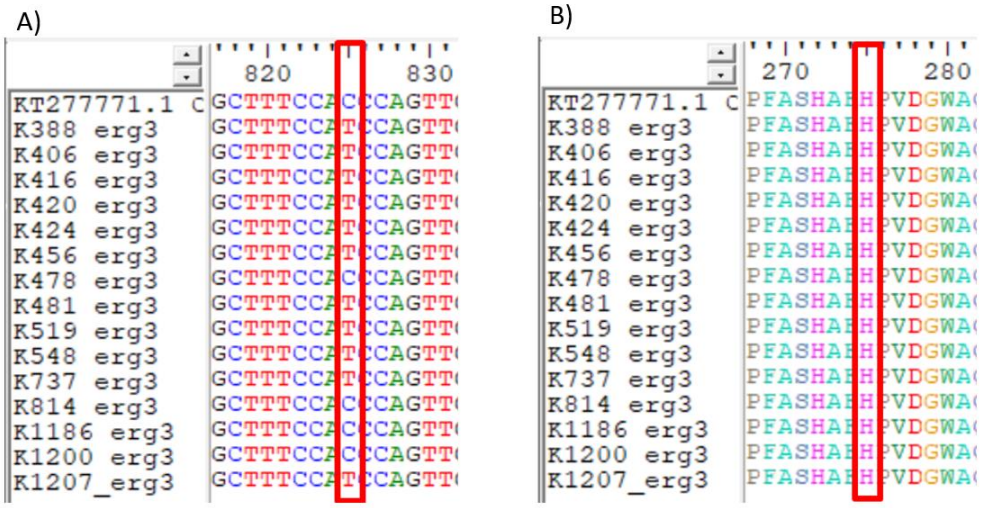

Figure 3.4: ERG3 gene C825T substitution A) nucleotide demonstration B) amino acid demonstration

3.3 Isolate selection for metabolomic and mRNA expressions

According to sequence analysis, five isolates whose have different point mutations in ERG11 gene, have been selected for the mRNA expression analysis and metabolite extraction(Table *3.6*).

Table 3.6:Selected isolates sequence and MIC results

Isolate Code	Mutation ERG11 gene	Mutation ERG3 gene	Fluconazole ug/ml	Voriconazole ug/ml	Posaconazole ug/ml
388	none	C825T	8	0,25	0,5
420	Y132F	C825T	8	0,125	0,125
1207	K143R	C825T	8	0,125	0,25
478	K143R+R398I	none	4	0,03	0,03
1186	Y132F+R398I	none	4	0,25	0,5

In selected isolates (according to their resistance mechanisms and point mutations) whose resistance genes are revealed, mRNA expression and metabolomic experiments were performed at control (0 MIC), 0.5 MIC, and 1 MIC fluconazole concentration exposure. Each of the chosen isolate for metabolomic and mRNA expression analysis was grown as three separate flasks until their control group growth curve reached the midpoint of the exponential phase. The midpoint of the exponential phase was determined by measuring the optical density (OD) at 550 nm for *C.parapsilosis*

ATCC 22019 as reference strain for selected isolates. Growth curve results were given in Figure 3.5.

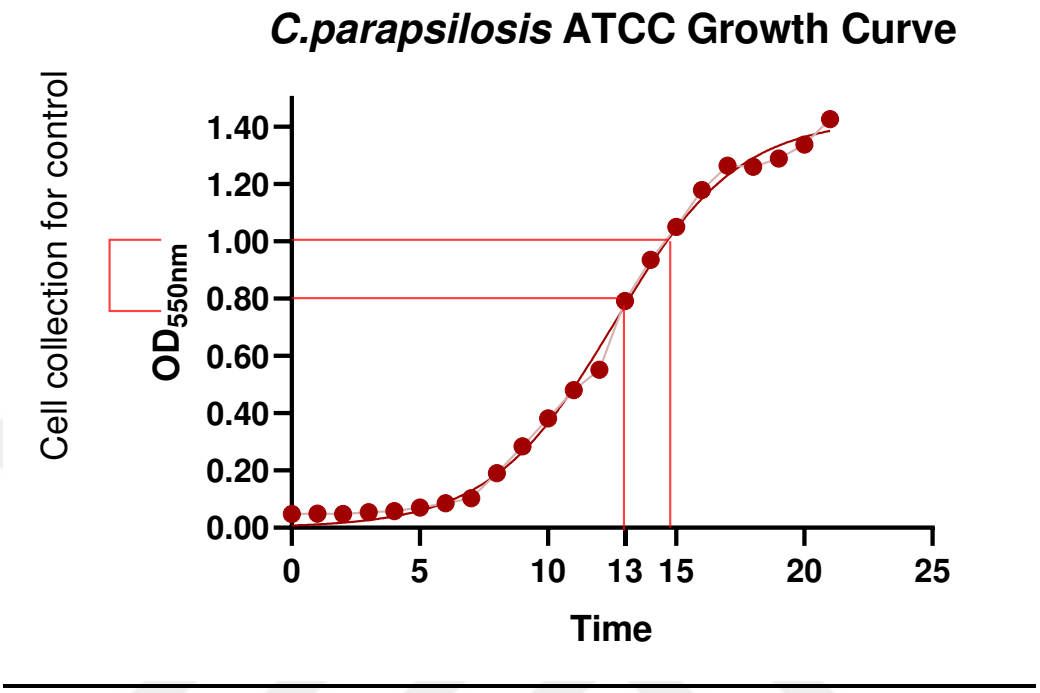

Figure 3.5:Growth kinetics of *C. parapsilosis* ATCC 22019

Once the control group (without fluconazole exposure) reached an OD550 nm of ≈0.8-1.0, cells from both the 0.5 MIC and 1 MIC fluconazole concentrations exposure groups were extracted for subsequent mRNA expression experiments and metabolomic studies, OD values were recorded during cell collection and given in Table *3.7*.

Table 3.7:OD550 nm values

No	FLU MIC	Control				0.5 MIC				1 MIC			
		Flask1	Flask2	Flask3	Mean	Flask1	Flask2	Flask3	Mean	Flask1	Flask2	Flask3	Mean
K388	8	0.732	0.778	0.782	0.764	0.723	0.720	0.730	0.724	0.619	0.587	0.638	0.615
K420	8	0.799	0.644	0.643	0.695	0.572	0.631	0.545	0.583	0.386	0.406	0.392	0.395
K1207	8	0.774	0.907	0.921	0.867	0.718	0.729	0.678	0.708	0.285	0.287	0.286	0.286
K478	4	0.977	0.986	1.005	0.989	0.288	0.446	0.425	0.386	0.204	0.183	0.143	0.177
K1186	4	0.857	1.080	0.917	0.951	0.513	0.544	0.625	0.561	0.361	0.341	0.373	0.358

3.4 mRNA expression alterations (Quantitative Real-Time Polymerase Chain Reaction)

3.4.1 RNA isolation Results

For the analysis of the mRNA expressions levels of selected Candida parapsilosis isolates according to their different mutations, first RNA of the samples were isolated as described in Section 2.5.1. The A260/230 values for extracted RNAs were ranged between 0.736-2.181 and the 260/280 values were detected as 2.192-1.837. RNA concentrations were between 177 ng/µl to 2297 ng/µl, these extracted RNAs were used for quantitative real time PCR.

3.4.2 Relative changes of mRNA expression for ERG11, ERG3 and UPC2

The table 3.9 displays the average fold changes that obtained with two sets of qPCRs in three important genes (ERG11, ERG3, and UPC2) between selected *C.parapsilosis* isolates exposed to different fluconazole concentrations (0 MIC, 0.5 MIC, and 1 MIC). All fold changes were calculated and presented in $2^{\Delta\Delta CT}$ form.

Table 3.8:Fold changes and SD of the ERG11, ERG3, UPC2 genes for the isolates under fluconazole exposure

K No	ERG11 Fold Changes (Av.)	±SD	ERG3 Fold Changes (Av.)	±SD	UPC2 Fold changes (Av.)	±SD
K388	11.081	1.609	0.091	0.041	0.682	0.041
K388(0.5 MIC)	24.520	0.968	0.211	0.015	1.135	0.013
K388 (1 MIC)	15.302	2.149	0.165	0.063	0.786	0.034
K420	2.757	0.336	0.156	0.014	1.228	0.271
K420(0.5 MIC)	5.164	0.033	0.312	0.067	2.217	0.957
K420 (1 MIC)	4.947	1.822	0.147	0.012	1.256	0.633
K478	41.792	6.832	7.126	0.663	42.571	2.809
K478(0.5 MIC)	14.282	0.363	6.154	0.298	7.627	0.583
K478 (1 MIC)	4.051	0.952	2.272	0.918	2.417	0.219
K1186	0.709	0.052	0.739	0.035	0.335	0.087
K1186(0.5 MIC)	3.132	0.631	1.935	0.237	1.901	0.752
K1186(1 MIC)	2.025	0.393	0.659	0.062	0.996	0.287
K1207	10.533	0.779	0.334	0.002	2.218	0.031
K1207(0.5 MIC)	5.308	0.655	0.203	0.060	2.147	0.907
K1207(1 MIC)	4.533	0.869	0.061	0.014	0.883	0.080

When we evaluated the changes in ERG11 gene expression of the isolates, isolate K388 showed a considerable rise in ERG11 expression compared to *C.parapsilosis* ATCC strain both in the presence and absence of fluconazole exposure. At the control group of K388 (0 MIC), ERG11 expression increased 11.08-fold, while at 0.5 MIC it increased 24.52-fold and at higher concentration (1 MIC) the expression slightly decreased to 15.30-fold change. In the K420 isolate, there was a 2.75-fold increase at 0 MIC, and it doubled to 5.20-fold for 0.5 MIC and at 1 MIC concentrations there were slightly decrease to 4.94-fold, similarly to K388. In the K478 isolate, noticeably it has the highest baseline (0 MIC) ERG11 expression of all the isolates with 41.79-fold change, it decreased to 14.28-fold and 4.05-fold at 0.5 MIC and 1 MIC concentrations, respectively under fluconazole exposure. When exposed to fluconazole, K1207 baseline comparatively high level of ERG11 expression (10.533 fold change) decreased to 5.30-fold at 0.5 MIC and 4.53 at the highest concentration (1 MIC).

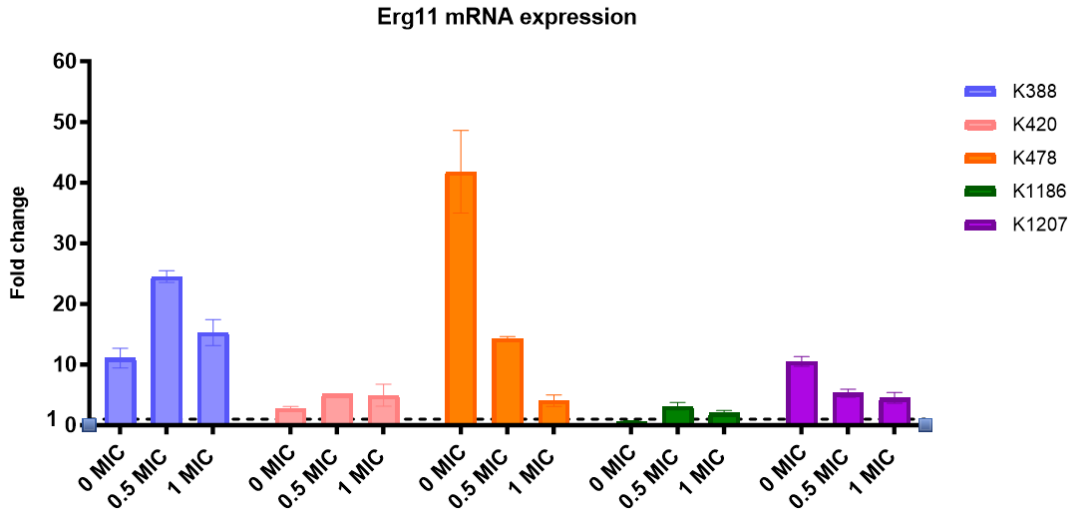

Figure 3.6:Fold changes of ERG11 mRNA expression for the fluconazole non-susceptible *C.parapsilosis* isolates

The response of ERG3 to fluconazole exposure was more varied between the isolates, and most of the isolates showed downregulation in the expression of ERG3. Strain K478 showed a substantial increase in expression at 0 MIC (7.12-fold), which decreased with higher fluconazole concentrations, it was 6.15-fold at 0.5 MIC and 2.27-fold at 1 MIC fluconazole exposure. This isolate (K478) showed decrease in fold changes under the fluconazole exposure for all ERG11, ERG3 and UPC2 genes.

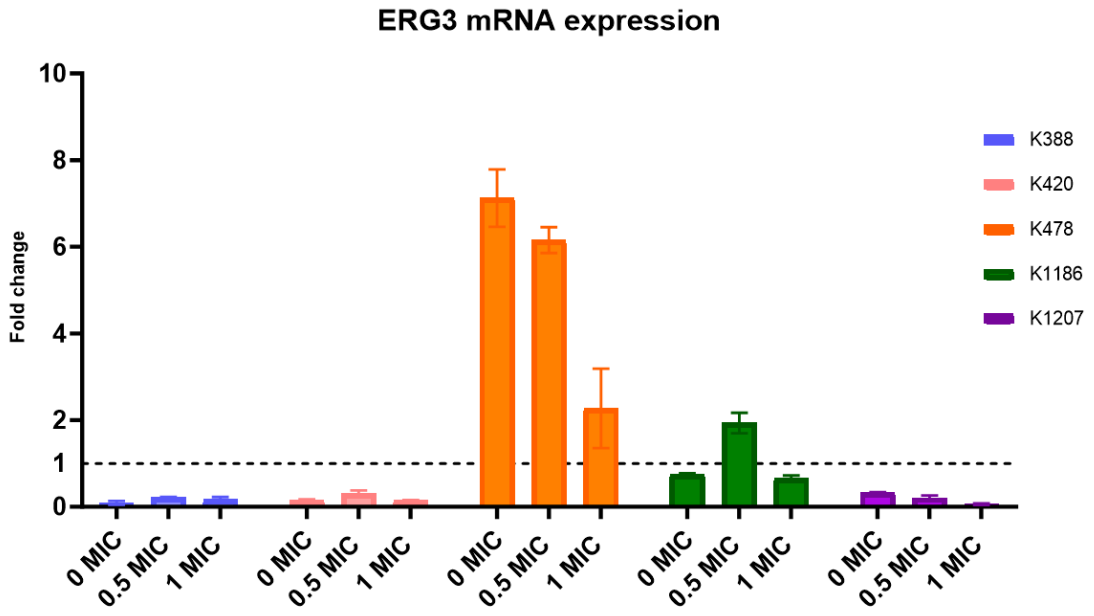

Figure 3.7:Fold changes of ERG3 mRNA expression for the fluconazole non-susceptible *C.parapsilosis* isolates

The isolates' responses to fluconazole exposure varied in terms of UPC2 gene expression. The baseline expression of K478 was significantly higher at 42.571 fold change, however it declined to 7.627-fold at 0.5 MIC and 2.417-fold at 1 MIC. K388's expression increased from 0.682 fold change at baseline to 1.135 at 0.5 MIC and 0.786 at 1 MIC. Expression of K420 increased from control (0 MIC) fold change of 1.228 to 2.217 at 0.5 MIC and then increased to 1.256-fold at 1 MIC. The expression of K1186 was 0.335 at baseline (0 MIC), rising to 1.901 at 0.5 MIC and stabilizing to 0.996 at 1 MIC. K1207's baseline expression was 2.218 at first, but it dropped to 2.147 at 0.5 MIC and then to 0.883 at 1 MIC.

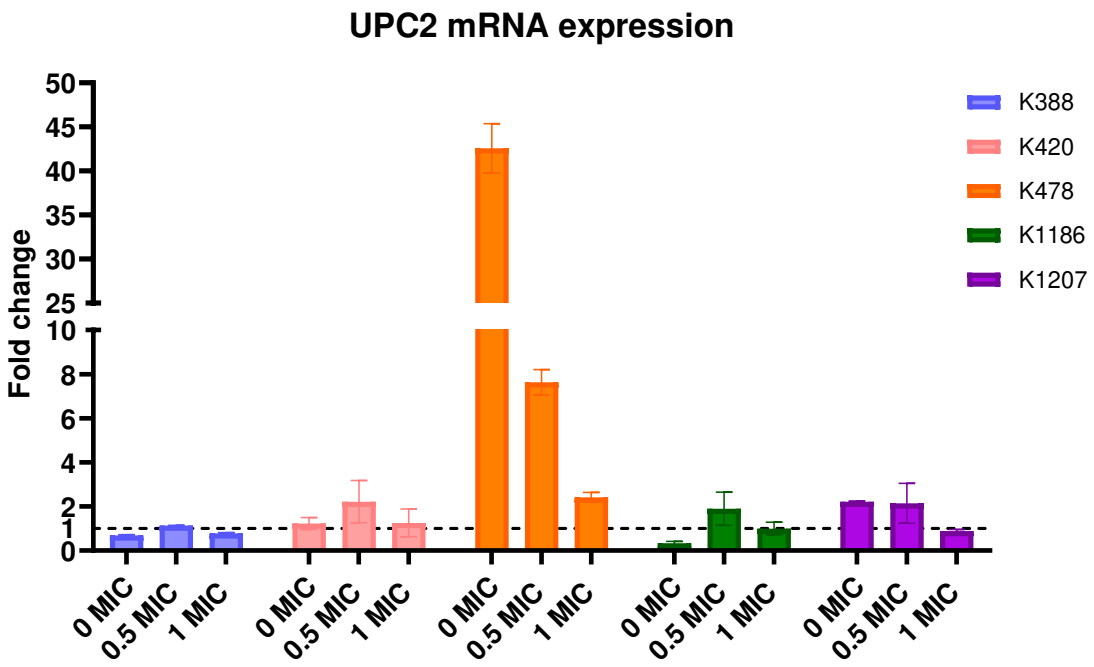

Figure 3.8:Fold changes of UPC2 mRNA expression for the fluconazole non-susceptible C.parapsilosis isolates

3.5 Metabolomic Analysis Results

For the metabolomic analysis, isolates alone PLS-DA graphs are composed, isolate K478 showed clear separation comparison between control vs. 0.5 MIC and control vs 1 MIC. Then to one step forward, PLS-DA graphic were composed by adding the other isolates one by one to K478 according to log transformation-mean centering, log transformation-auto scaling, log transformation-pareto scaling, log transformation-range scaling(Table 3.9), square root transformation-mean centering, square root transformation-auto scaling, square root transformation-pareto scaling, square root transformation-range scaling(Table 3.10), cube root transformation-mean centering, cube root transformation-auto scaling, cube root transformation-pareto scaling, cube root transformation-range scaling(Table 3.11) with the help of online metabolomics statistical analysis tool MetaboAnalyst 5.0.

According to results, K478+K420, K478+K1186, K478+K1207 showed visual discrimination on the PLS-DA graphs when the analysis is performed according to log transformation -auto scaling. Analysis are performed by increasing the sample pool, for this reason K478+K420+K1186, K478+K420+K1207, K478+ K1186+K1207 groups are generated and PLS-DA graphics are created with using log transformation -auto scaling method. By this method, the most visually discriminated isolates are grouped as K478+K420+K1207 and K478+K1186+K1207 according to their fluconazole exposure as control and 1 MIC fluconazole groups.

Table 3.9: Log transformation based analysis for different groups

Sample	Comparison group	Log transformation-mean centering	Log transformation-auto scaling	Log transformation-pareto scaling	Log transformation-range scaling
K478+K388	Control vs 0.5 MIC	none	none	none	none
	Control vs 1 MIC	seperated(partial)	none	none	none
K478+K420	Control vs 0.5 MIC	none	seperated(clear)	none	none
	Control vs 1 MIC	none	seperated(clear)	seperated(clear)	seperated(clear)
K478+K1186	Control vs 0.5 MIC	none	seperated(clear)	none	slight seperation
	Control vs 1 MIC	seperated(clear)	seperated(clear)	seperated(partial)	seperated(partial)
K478+K1207	Control vs 0.5 MIC	none	seperated(clear)	none	seperated(clear)
	Control vs 1 MIC	seperated(clear)	seperated(clear)	seperated(clear)	seperated(clear)
K478+K420+K1186	Control vs 0.5 MIC	NA*	slight seperation	NA*	NA*
	Control vs 1 MIC	NA*	slight seperation	NA*	NA*
K478+K420+K1207	Control vs 0.5 MIC	NA*	no seperation	NA*	NA*
	Control vs 1 MIC	NA*	seperated(clear)	NA*	NA*
K478+K1186+K1207	Control vs 0.5 MIC	NA*	seperated(partial)	NA*	NA*
	Control vs 1 MIC	NA*	seperated(partial)	NA*	NA*

*For the analysis with three isolate, auto scaling which has showed clear discrimination for two isolates in PLS-DA is used

Table 3.10:Square root transformation based analysis for different groups

Sample	Comparison group	Square root transformation-mean centering	Square root transformation-auto scaling	Square root transformation-pareto scaling	Square root transformation-range scaling
K478+K388	Control vs 0.5 MIC	none	none	none	none
	Control vs 1 MIC	none	none	none	none
K478+K420	Control vs 0.5 MIC	none	seperated(clear)	none	none
	Control vs 1 MIC	slight seperation	seperated(clear)	seperated(partial)	seperated(clear)
K478+K1186	Control vs 0.5 MIC	none	seperated(partial)	none	none
	Control vs 1 MIC	seperated(clear)	seperated(clear)	seperated(clear)	seperated(partial)
K478+K1207	Control vs 0.5 MIC	none	seperated(clear)	none	seperated(partial)
	Control vs 1 MIC	seperated(clear)	seperated(clear)	seperated(clear)	seperated(clear)
K478+K420+K1186	Control vs 0.5 MIC	NA*	slight seperation	NA*	NA*
	Control vs 1 MIC	NA*	slight seperation	NA*	NA*
K478+K420+K1207	Control vs 0.5 MIC	NA*	no seperation	NA*	NA*
	Control vs 1 MIC	NA*	seperated(clear)	NA*	NA*
K478+K1186+K1207	Control vs 0.5 MIC	NA*	slight seperation	NA*	NA*
	Control vs 1 MIC	NA*	seperated(partial)	NA*	NA*

*For the analysis with three isolate, auto scaling which has showed clear discrimination for two isolates in PLS-DA is used

Table 3.11:Cube root transformation based analysis for different groups

Sample	Comparison group	Cube root transformation-mean centering	Cube root transformation-auto scaling	Cube root transformation-pareto scaling	Cube root transformation-range scaling
K478+K388	Control vs 0.5 MIC	none	none	none	none
	Control vs 1 MIC	none	none	none	none
K478+K420	Control vs 0.5 MIC	none	seperated(clear)	none	none
	Control vs 1 MIC	slight seperation	seperated(clear)	seperated(partial)	seperated(clear)
K478+K1186	Control vs 0.5 MIC	slight seperation	seperated(clear)	slight seperation	slight seperation
	Control vs 1 MIC	seperated(clear)	seperated(clear)	seperated(partial)	seperated(partial)
K478+K1207	Control vs 0.5 MIC	none	seperated(clear)	none	seperated(clear)
	Control vs 1 MIC	seperated(clear)	seperated(clear)	seperated(clear)	seperated(clear)
K478+K420+K1186	Control vs 0.5 MIC	NA*	slight seperation	NA*	NA*
	Control vs 1 MIC	NA*	no seperation	NA*	NA*
K478+K420+K1207	Control vs 0.5 MIC	NA*	no seperation	NA*	NA*
	Control vs 1 MIC	NA*	slight seperation	NA*	NA*
K478+K1186+K1207	Control vs 0.5 MIC	NA*	slight seperation	NA*	NA*
	Control vs 1 MIC	NA*	slight seperation	NA*	NA*

*For the analysis with three isolate, auto scaling which has showed clear discrimination for two isolates in PLS-DA is used

3.5.1 PLS-DA graphics and VIP score plots of selected groups and isolates

Group one: (K478+K420+K1207)

All groups were generated by adding one- by- one until detecting visual discrimination in the partial least squares-discriminant analysis (PLS-DA) graphics. By this method, first group of the isolates is K478+K420+K1207 is obtained, and results are given below (Figure 3.9). K478+K420+K1207 isolate group control (without fluconazole exposure) and 1 MIC fluconazole exposure group is analysed with PLS-DA score plot, results are showing very clear clustering of control and 1 MIC groups. The same-colored circles represent replicates of metabolic profiles for each group in the PLS-DA plot. The colored ellipses indicate 95% confidence regions of each group. According to VIP score plot, Homocysteine, NADP+, Arginine, Methionine, Beta-Alanine, N-aceytlyaspartate were decreased in 1 MIC fluconazole exposure compared to control group.

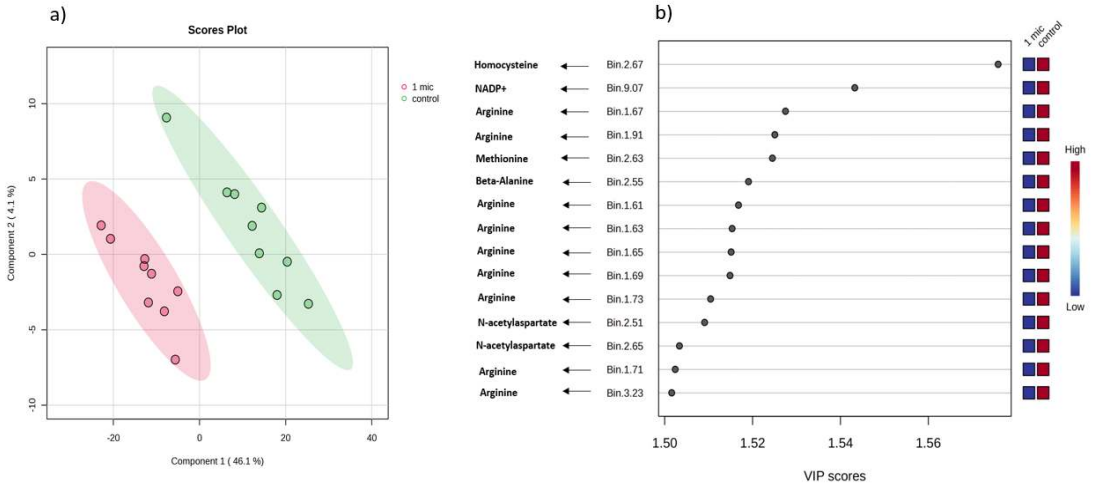

Figure 3.9:a)Partial least squares-discriminant analysis (PLS-DA), b)VIP scores plot showing control vs.1 MIC fluconazole treatment for the isolates K478+K420+K1207

Group two: (K478+K1186+K1207)

PLS-DA graphics are obtained until detecting visual discrimination by adding one- by-one. Second group of the isolates K478+K1186+K1207 is obtained with this method, and results are given below (Figure 3.10). K478+K1186+K1207 isolate group control (without fluconazole exposure) and 1 MIC fluconazole exposure group is analysed with PLS-DA score plot, results are showing clear clustering of control and 1 MIC groups. The same-colored circles represent replicates of metabolic profiles for each group in the PLS-DA plot. The colored ellipses indicate 95% confidence regions of each group. Arginine, Methionine, N-aceytlaspartate, Arabinitol were decreased in 1 MIC fluconazole exposure compared to control group.

In our study the metabolic pathways most significantly altered are :1)alanine, aspartate, and glutamate metabolism; (2) arginine and proline metabolism, 3) homocysteine, methionine metabolism and 4) arabinitol metabolism.

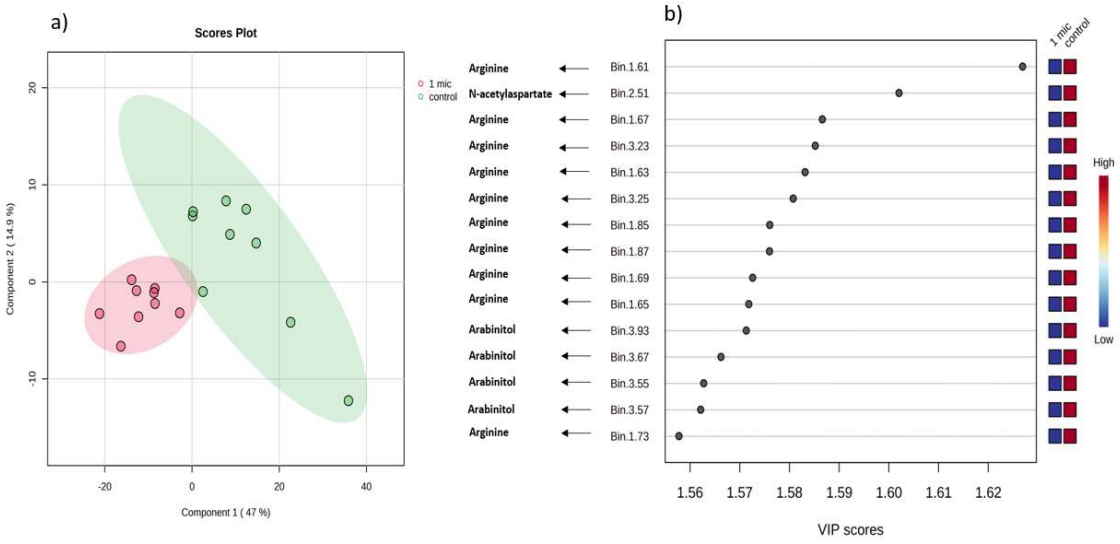

Figure 3.10:a)Partial least squares-discriminant analysis (PLS-DA), b)VIP scores plot showing control vs.1 MIC fluconazole treatment for the isolates K478+K1186+K1207

Chapter 4:
DISCUSSION

The World Health Organization (WHO) has recently prioritized international surveillance for the identification and management of fungal infections, as *Candida* infections are becoming increasing concern. *C. parapsilosis* is one of the pathogen that took place in the list(WHO, 2022).

C. parapsilosis complex is the second most common species that causes bloodstream infection among *Candida* especially in immunocompromised patients, neonates both in our country and in Southern Europe. While *Candida albicans* is still the most common species to be seen, recent epidemiological studies draw attention to increasing incidence of non-albicans species. *C.parapsilosis* is one of these important non-albicans species due to their tendency to develop strong biofilms on medical catheters and implants (Tóth et al., 2019).Distribution of *Candida* species, are affected from many factors such as patient age, antifungal exposure, comorbidities, geographic region, and hospital infection control policies (Guinea, 2014).

Together with the high isolation rates of *C. parapsilosis* from candidemia patients, it is concerning that floconazole resistance in *C. parapsilosis* has been identified in numerous locations worldwide. Azole group therapies are recommended primarily because they are more affordable and have a more limited range of adverse effects (Pappas et al., 2016). Reports of emerging resistance to fluconazole have come from Turkey(26.4%) , Greece, Italy(33%), Brazil(67.9%), Saudi Arabia(33%), India, and South Korea, Mexico(54%), Soth Africa(54%)(Escribano & Guinea, 2022; Magobo et al., 2020; Martini et al., 2020; Thomaz et al., 2018) So, evaluating the azole resistance by molecular methods of *C. parapsilosis* becomes extremely important.

In this study, we examined 15 fluconazole-non-susceptible *C. parapsilosis* isolates isolated from blood cultures from three different universities and state hospitals between 2016 and 2018. Antifungal susceptibility testing showed that all isolates were non-susceptible to fluconazole, 47% were non-susceptible to voriconazole, and 33% were non-wild type to posaconazole. These findings highlight the 33% of the isolates were found to be resistant to all azoles, and this pan-azole resistance is an important finding that seriously limits clinical treatment options. In the literature azole resistance rate in

Turkey was found to be between 0%-47.1%.(Arastehfar et al., 2020; Arikan-Akdagli et al., 2019; Escribano & Guinea, 2022)

The primary mechanism that causes azole resistance in *C. parapsilosis* is point mutations in the active region of the ERG11 gene, gene which encodes the enzyme lanosterol 14α-demethylase. In our study sanger sequencing results on the ERG11 gene revealed that 66% of the isolates carried the Y132F mutation in the ERG11 gene. Mutations in ERG11 gene is the most common mutation associated with resistance to fluconazole all over the world and was determined to be the main cause of fluconazole resistance in *C. parapsilosis* isolates in this study. The Y132F mutation is of critical importance in understanding the molecular basis of resistance of *C. parapsilosis* isolates to antifungal drugs.

In a worldwide fungal surveillance study, it is found that 89.1–91.6% of *C. parapsilosis* isolates susceptible to azoles, and most resistant isolates found in Europe(15.1%), 34 of the 36 isolates from Italy was carrying Y132F mutation in their ERG11 gene(Castanheira et al., 2020).

According to the recent reports, Y132F mutants also have tendency to persistence in hospital environments and have higher propensity to cause clonal transmission and more likely to belong to a cluster than other *C. parapsilosis* isolates(Arastehfar et al., 2021; Choi et al., 2018; Magobo et al., 2020). As a result, these resistant isolates become the dominant *C. parapsilosis* clone in the hospital setting and persist for a long period of time on the surface of medical devices, patient rooms and causes life treating infections in immunocompromised patients. According to our results, while the Y132F mutation was detected alone in eight of the ten isolates carrying Y132 F (+), the Y132F mutation was detected together with the R398I mutation in the other two isolates (K1186:MIC 4 ug/ml; K1200: MIC 4 ug/ml).

The K143R mutation in ERG11 was detected in two isolates (K478 and K1207) in our cohort. According to Xiang et al. (Xiang et al., 2013) mutations at position K143 may prevent the inhibitor or substrate from entering the active site or from binding to it. This mutation was detected alone in one of them (K1207), and in the other isolate (K478), the K143R mutation was detected together with the R398I mutation. Both of the isolates were resistant to fluconazole and susceptible to voriconazole and posacanozole. In a study performed with *C.albicans*, the azole-susceptible *C. albicans* strain was mutated K143R homozygously, leading to the strongest decrease in fluconazole susceptibility; however voriconazole susceptibility was only slightly effected(Flowers et al., 2015).In the

literature, the K143R is one of the most frequently detected mutations, either together with the Y132F mutation or alone. However in our cohort we did not detected K143R mutation in our Y132F mutants. In another study performed with *C.parapsilosis* isolated from Turkey, they found the fluconazole resistance rate as %27(60/225) and among these isolates 24 were harbouring Y132F mutation alone in ERG11 gene, and 19 of them was carrying Y132F mutation together with K143R(Arastehfar et al., 2020).

In our study, R398I mutation have been detected together with other important mutations (Y132F, K143R) but was not detected in alone. In previous two studies performed in US showed nearly all fluconazole susceptible and fluconazole resistant *C. parapsilosis* isolates were found to have the R398I mutation in combination with the Y132F substitution mutation. These previous studies indicated that the R398I mutation lesser importance for azole resistance since it was identified in fluconazole susceptible isolates, also when this mutations is observed in fluconazole non-susceptible isolates it observed with the combination of other missense mutations(Choi et al., 2018; Khalifa et al., 2024).

In ERG3 sanger sequences results showed that there was silent mutation in nucleotide C825T. No there was no study explain the relation of this polymorphism and the azole resistance in the literature.

In addition to these mutations, expression changes (decrease/increase) in genes encoding enzymes related to ergosterol synthesis are also thought to be important in resistance. Changes in the expression levels of the target enzyme is another significant mechanism for drug resistance in Candida species. The activation of numerous important genes, such as ERG11, ERG3, and UPC2, is intimately linked to the development of resistance to azole antifungals in *C. parapsilosis.* Studies have shown that in addition to point mutations in ERG11 in Candida species , 2-fold increase in ERG11 gene mRNA level of Y132F positive isolates was found(Berkow et al., 2015).

In our study, we examined the ERG11 mRNA expression levels and found that ERG11 expression was always found to be upregulated in isolates carrying different mutations other than K1186 control (0 MIC). An increase in ERG11 expression is observed regardless of the mutation type. It is observed that different fold changes obtained under fluconazole exposure depending on the mutation type, strain specific responses have been observed as we seen in Figure 3.6, Figure 3.7, Figure 3.8. Daneshnia et. al. also found similar upregulation results in ERG11 mRNA expression levels under fluconazole exposure regardless of the susceptibility and mutations in ERG11 genes, and

they argued that mutations may limit the Erg11 enzyme's catalytic activity, implying that the rise in basal expression that has been seen may be a strategy to compensate for the lower ergosterol synthesis(Daneshnia et al., 2022).

The isolate K478 which has K143R and R398I but not Y132F mutations is demonstrated by the notable rise in ERG11 expression before to fluconazole exposure, which subsequently declined after the drug was applied. This decline also observed both in ERG3 and UPC2 mRNA expression levels. Silva et al. also observed 2.69 fold decrease in ERG11 mRNA expression of fluconazole induced azole-resistant *C.parapsilosis* isolates, 2.01 fold decrease in voriconazole induced azole resistant cells(Silva et al., 2011).This total decline both transcription activator (UPC2) and end targets (ERG11 and ERG3) in our K478 isolate would suggest an adaptation process to azole stress and should be further examined with deeper metagenomic technics. In particular, isolate K388 which has no mutation in ERG11 gene showed upregulation of ERG11 expression under 0.5 MIC fluconazole exposure (2.2 times higher), this upregulation also detected under 1 MIC fluconazole exposure (1.4 times higher). This data somewhat agrees with results reported in the literature, where azole resistance has frequently been linked to ERG11 overexpression. Souza et al were found that ERG11 mRNA expression was 1.5 to 7.4 times higher in fluconazole-resistant *C.parapsilosis* isolates containing the point mutation(Souza et al., 2015). Also Silva et al found an increase in transcription factors related to ergosterol biosynthesis after exposure to azole drugs(Silva et al., 2011). Hence, K478 is a non-Y132F mutant and harbours K143R mutation, the mRNA expression profiling study with a larger cohort of non-Y132F mutants should be implemented to understand the different behavior of these isolates under drug pressure.

Zinc cluster member transcription factor family known as Sterol Uptake Control Protein 2 (Upc2) partially controls the enzymes involved in the sterol production pathway. When sterol levels in the yeast are reduced, for example from fluconazole interference, Upc2p detects the sterol levels and activates the genes involved in sterol absorption and production. Sensing the sterol levels is important for the fungal lipid homeostasis(Bandara et al., 2020). Most of the sterols are located in the cell and nuclear membranes, a very small amount is found free in the cytosol. When UPC2 detects sterol depletion in the cytosol UPC2 is transported to the nucleus behave as a transcriptomic up regulator and it increases the activity of genes involved in sterol biosynthesis (Tan et al., 2022). UPC2 deletion can cause increased antifungal susceptibility in *Candida* species. Inability of the homozygous deletion strains to the upregulation of ergosterol biosynthesis

related genes such as ERG2 and ERG11 can result increased susceptibility to membrane sterol inhibitors drugs such as azoles.

In a study that performed by Silver et. al., they used homozygous deleted of UPC2 in *C. albicans* and they showed increase in the expression of ERG2 and ERG11 for all strains except UPC2 deleted strain when the cells are grown under fluconazole pressure. So, these results suggest the UPC2 gene regulates the expression of the ERG11 gene. They have also discussed that UPC2 deleted strains have lower level of ergosterol reservoir. Slow replacement process of existing ergosterol reserves in UPC2 deleted strains leads to increased susceptibility to drugs targeting ergosterol synthesis. Also, they suggests UPC2 plays a crucial role in the uptake or retention of lipophilic molecules. The decrease in lipophilic molecules may restrict the cell's uptake of sterols from outside. This prompting the cells an increase in gene expression to compensate by synthesizing sterol via UPC2. Deleted cells are in capable of produce their own sterol or take it from outside; this leads to sterol deficiency and consequent disruption of the cell membrane, cells become more vulnerable to osmotic stress(Silver et al., 2004).

In another study, Dunkel et. al compared the transcriptional profiles of fluconazole susceptible and fluconazole resistant two isolates and they found upregulation in several genes related with the ergosterol biosynthesis together with the UPC2 which is encodes transcription factor responsible for the regulation of ergosterol biosynthesis genes and induces their expression(Dunkel et al., 2008).

A study by Feng et al. showed that when susceptible and resistant isolates were compared, ERG3 expression was higher in susceptible isolates. However, it revealed that ERG3 expression was reduced in resistant isolates(Feng et al., 2019). In our studies, we observed a similar downregulation in ERG3 gene expression for most of the isolates. Even when we exposed to cells different concentration of azole (0.5 MIC and 1 MIC) downregulation of the ERG3 expression observed. However, isolate K478 showed upregulation in ERG3 expression even under the 0.5 MIC and 1 MIC fluconazole exposure. It is thought that this effect may be related to the general transcriptomic activator effect of UPC2 on all sterol-related genes. Hence, K478 was the isolate that highest UPC2 expression levels were detected.

In a study performed by Rybak et.al, it was stated that the ERG3 Mutant (G111R) contributes to azole resistance by reducing sterol desaturase activity. Additionally, when they performed gene transformation by transferring the genes carrying this mutation into a wild-type isolate, they observed a decrease in sterol desaturase activity in the newly

created mutant *C. parapsilosis* cells (Rybak et al., 2017). This leads to high levels of azole resistance. However, in our study, no significant mutations were shown other than missense mutation. To sum up, the mRNA expression levels of ERG11, ERG3 and UPC2 genes in fluconazole non-susceptible *C.parapsilosis* isolates varies according to ERG11 mutations and shows strain specific responses to fluconazole exposure.

Metabolomics together with associated bioinformatic tools, provides a deeper understanding of the metabolic responses of fungal infections by directly exposing the effects of cellular activity. Unlike transcriptomics that helps to understands variations in gene expressions, this methodology reveals detailed downstream effects of cellular processes, so facilitating a better understanding of metabolic regulation, environmental adaption, and stress responses and reporting picture of organismal responses at the molecular level. This comprehensive perspective is improving our knowledge by unraveling the complex biochemical processes, it is important to better understanding of the pathogenicity and survival of fungi. This may lead to the identification of new targets for antifungal therapies(Brandt et al., 2020).

Fungal pathogenicity is largely attributed to their extraordinary metabolic adaptability. Because of this characteristic, fungus can grow by using a variety of anabolic and catabolic pathways to switch between carbon and nitrogen sources as needed for metabolism(Neelu Begum et al., 2022).

However, the use of metabolomics methods to investigate antifungal resistance in *Candida* is still rare. Azole group drugs stop the synthesis of ergosterol at various stages, creating intracellular toxic metabolites(D. Sanglard et al., 2003). When the function of 14-α demethylase is inhibited, ERG3 plays an important role for converting nontoxic sterol intermediates into the toxic sterol 14α-methyl-ergosta-8,24(28)-dien-3,6-diol. Inactivation or loss of this enzyme can cause increase in nontoxic ergosta-7,22-dienol. (Rybak et al., 2017). However, the destructive effect of toxic metabolites on the cell and the metabolomic processes created in response to azole exposure in *Candida* species are not yet known.

In our study we analyzed the changes of intracellular metabolites of *C. parapsilosis* isolates which have different mutations under the fluconazole exposure by NMR spectroscopy method. According to our analysis for the isolate group K478+K420+K1207; homocysteine, NADP+, arginine, methionine, beta-Alanine, N-aceytlyaspartate and for the isolate group K478+K1186+K1207; arginine, methionine, N-

aceytlaspartate, arabinitol were decreased in 1 MIC fluconazole exposure compared to control group for both isolate group.

Our results showed that under the fluconazole exposure, the metabolic pathways most significantly altered are :1) alanine, aspartate, and glutamate metabolism; 2) arginine and proline metabolism, 3)homocysteine, methionine metabolism and 4) arabinitol metabolism.

Our results are indicating that the fundamental changes observed in our study are closely related to two important biochemical processes which are nitrogen assimilation and oxidative stress responses. The first of these processes is nitrogen assimilation. Because of this process, when glycogen sources decrease, *Candida* can use amino acids and precursors related to nitrogen metabolism in energy metabolism. This allows amino acid metabolism to be proposed as an alternative energy source in stress responses and alternative carbon sources for growth. (N. Begum et al., 2022). The research conducted by Gallo et al. provides useful information on the metabolic flexibility of *C. albicans* in response to many environmental circumstances, with a particular emphasis on nutrient availability. This work illustrates how *C. albicans* changes its metabolism both intracellular and extracellular to varied temperatures and environmental conditions using 1H-NMR spectroscopy. According to their finding's most altered metabolisms were alanine, aspartate, and glutamate metabolism; arginine and proline metabolism; glycerolipid metabolism. Some amino acids such as proline are consumed more in the medium with a lower carbon source, suggesting it enters the metabolic pathways responsible for nitrogen assimilation and/or its conversion to glutamate. They revealed that *C. albicans* exhibits its metabolic flexibility by transitioning to different metabolic pathways when glucose is ends(M. Gallo et al., 2022; Schaefer et al., 2020).

Similar to our study, Katragkou et al. investigated the effects of fluconazole on the metabolomic profile of *C. albicans* but differently they examined the metabolomic changes by using LC/MS-based metabolomic profiling. Significant metabolic changes are shown by their research, most notably in the pathways involved in amino acid synthesis and central carbon metabolism. More specifically, 64 metabolites have been identified and of those abundance of 12 metabolites has changed under the fluconazole exposure. The main findings include elevated concentrations of mevalonate and the intermediates of central carbon metabolism (a-ketoglutarate, glucose-6-phosphate, phenylpyruvate, and ribose-5-phosphate). On the other hand, there were decreases in numerous amino acids guanine and five other amino acids (glycine, proline, tryptophan,

aminoisobutanoate, and asparagine) were less abundant, which highlighted the metabolic impact caused by fluconazole exposure. These alterations suggest a strategic metabolic reprogramming by *C. albicans* to counteract the effects of fluconazole, potentially contributing to the fungus's survival. Researchers are discussed that metabolomic changes are not only for the survival, but they also imply that the heightened activity observed in the mevalonate pathway could potentially occurred due to inhibitory effects of fluconazole on the downstream formation ergosterol, hence contributing to the development of fluconazole resistance. By blocking the carbon flow to ergosterol, an antifungal drug that blocks a step in the sterol biosynthesis pathway should increase the byproducts of the mevalonate process(Hornby & Nickerson, 2004; Katragkou et al., 2016).

The findings suggest that the decrease observed in alanine, arginine and aspartate levels under fluconazole exposure as a result of depletion of the glucose source may be related to nitrogen assimilation. Running out of a key carbon source such as glucose requires *Candida* to turn to alternative pathways to obtain energy. In this process, amino acids and related compounds can be used to provide energy and structural components of the cell. The decrease in specific amino acids such as alanine, arginine and aspartate indicate that these molecules are used in energy production and are part of the cell's adaptation mechanisms under stress.

In-depth proteome analysis of *C. albicans'* adaptation to the stress of fluconazole exposure is presented in the Song et. al. Liquid chromatography-tandem mass spectrometry (LC-MS/MS) and tandem mass tag (TMT) labeling combined, and study offers excellent insights into the intricate metabolic alterations that occur in response to antifungal pressure, particularly when fluconazole resistance is emerging. Specifically in strains with increased fluconazole resistance. They found upregulation in amino acid metabolism and downregulation in the metabolism of carbohydrates and lipids. This change indicates a strategic metabolic shift that may be made to offset the energy deficiency and increased requirements for biosynthesis come with the fluconazole stress(Song et al., 2022).According to their findings many proteins involved in cysteine and methionine metabolism were increased in fluconazole susceptible *C. albicans* cell.

D-arabinitol (DA), a five-carbon sugar alcohol, is a metabolic byproduct predominantly produced by most pathogenic *Candida* species. In clinical research, notably among immunocompromised patients, often those with neutropenia, experiencing invasive candidiasis, an increase in DA to L-arabinitol (LA) or DA to

creatinine ratios in serum or urine has been documented. Furthermore, the detection of DA preceded positive outcomes in blood cultures by several days to weeks, with a return to normal DA levels being indicative of a positive therapeutic response(Christensson et al., 1999a, 1999b). The initial efforts to utilize DA measurements for diagnostic purposes throughout the 1990s yielded variable results in terms of sensitivity and specificity. Subsequent clinical studies aimed to assess the diagnostic and prognostic utility of arabinitol quantification, reflecting the ongoing exploration into its clinical relevance (Wells et al., 1983). Due to the factors related with the restricted accessibility of metabolomic arrays in routine laboratories, D-arabinitol test has not yet been widely availability due to the restricted accessibility of the metabolomic assays in routine laboratories, it still holds promise as a novel diagnostic tool for invasive candidiasis. In a study, Kayingo et al, examined the D-arabinitol response under environmental stress and found that elevated temperature and high H_2O_2 levels triggers the synthesis of arabinitol (Kayingo & Wong, 2005), Consistently, Gallo et al found that, under starvation and hypo-osmotic stress *Candida* release intracellular substances such as arabinitol to overcome this stress(Mariana Gallo et al., 2022). Similarly, in our study we found that, under 1 MIC concentration of fluconazole exposure, the arabinitol levels significantly decreased as a response to osmotic pressure caused by disruption of cell membrane due to the azole activity.

According to literature, susceptibility of the yeast to different antifungals affected from the changes in the cysteine biosynthesis. The reduction of glycine in *C. albicans* cells treated with fluconazole is likely partially due to oxidative damage as a result of the decreased synthesis of intracellular glutathione(Kim & Fay, 2007).

Methionine which is the one of the four common sulfur containing amino acids (methionine, homocysteine, taurine, cysteine) is required for normal growth. On the surface proteins it serves as an endogenous antioxidant and in prokaryotes and eukaryotes methionine has role as an initiator of protein synthesis. Also, by sustaining several metabolic pathways, methionine metabolism performs significant roles (Parkhitko et al., 2019). Methionine serves as a precursor for S-adenosyl methionine (SAM), which is a chemically varied compound engaged in a variety of processes, including aminopropyl donation in polyamine production and methylation in the biosynthesis of ergosterol (Song et al., 2022). In a study that investigated the metabolomic changes of *C. albicans* cells when they treated with Amphotericin B (AmB) performed by Cao. Et. al indicate that higher levels of spermidine and spermine, two important polyamines in eukaryotes, may

shield *C. albicans* cells from the effects of antifungal agents, which may be linked to a reduction in the build-up of reactive oxygen species. Similar to our study they have also found that arabinitol level is decreased in AmB-treated cells (Cao et al., 2013).

In a study that investigates the metabolomic differences in *Candida* species, Beagum et. al. revealed that *C.albicans, C.glabrata* and *C.auris* (AGAu) species used amino acid metabolism which included the metabolism of cysteine, methionine, and arginine, potentially enhancing their competitive fitness in pathogenesis. In the choline pathway, fatty acid biosynthesis and polyamine pathway showed elevated levels of metabolites in AGAu species. The main mechanisms that propagate these pathways are the methionine, cysteine, and arginine pathways (Neelu Begum et al., 2022). In our study when *C.parapsilosis* cells were exposed to 1 MIC concentration of fluconazole, we observed decreased level of the methionine, homocysteine and arginine levels.

Choline, fatty acid, and polyamines like spermidine and spermine are especially found in and essential for the cell membrane. The observed decrease in methionine, cysteine and arginine levels may be related to response of changes in membrane structure as a result of fluconazole exposure, this may explain the decrease in amino acids associated with these pathways. This may be related with the remodeling and neutralizing the changes of the cell membrane structure. In this context, it is possible that fluconazole exposure triggered the decrease in arginine, homocysteine and methionine levels. Considering that fatty acid biosynthesis supports functions critical to pathogenesis, such as fungal cell membrane viability, energy storage, signaling, and cell proliferation, maintaining and modulating the activity of these pathways is vital for understanding the azole resistance mechanisms.

This study represents one of the rare studies in the literature that evaluates the behavior of Candida species under azole pressure from a metabolomics perspective. Our findings indicate that significant changes occur, especially in energy metabolism. Considering the mechanism of action of azoles, significant metabolomic changes in cell membrane structure are also important.

Our study is designed as a small pilot study for revealing the effect of fluconazole exposure on drug resistant *C.parapsilosis* isolates which are harboring different point mutations in ergosterol synthesis pathway key enzyme genes. As a pilot study, the main limitation of our study is the sample size. Our result should be confirmed with higher numbered cohort studies. In our study we investigated the ergosterol synthesis related genes expression and mutations. However, there are other mechanisms related with the

azole resistance such as efflux pumps(CDR1 from the ABC- transporter family, MDR1 from the MFS-transporter family), mutations in TAC1 and MRR1 genes and genomic variations that includes loss of heterozygosity and aneuploidy. Also, the information obtained through metabolomic analysis reflects only a fraction of the current knowledge. Therefore, it is important to strengthen the study with broader sample size and comprehensive omics studies integrating lipidomic analysis.

Finally, although these strategies contribute to the survival of the fungus, the effects of resistance mechanisms on mortality and their clinical significance have not yet been clearly determined, and more comprehensive cohort studies are needed in these aspects.

Chapter 5:
CONCLUSION

In conclusion, *C.parapsilosis* is serious healthcare problem, together with the increasing azole resistance rates. This study helps to understand the azole resistance machanisms by investigation of the expression of key enzymes genes in ergosterol synthesis and metabolomic changes under fluconazole pressure in drug resistant C. parapsilosis isolates. Our results shows strain specific mRNA expression patterns in genes associated to the ergosterol biosynthesis pathway. This response variability highlights the complex nature of resistance mechanisms, which go beyond straightforward mutations in the ERG11 and ERG3 genes. According to metabolomic analysis results, under the fluconazole exposure, the metabolic pathways most significantly altered are :1) alanine, aspartate, and glutamate metabolism; 2) arginine and proline metabolism, 3) homocysteine, methionine metabolism and 4) arabinitol metabolism. These metabolomic changes observed in our study might be related with the cellular strategy to counteract fluconazole's toxicity and to promote survival. A detailed in-depth investigation of this survival response will uncover new drug targets in the future.

BIBLIOGRAPHY

Akins, R. A. (2005). An update on antifungal targets and mechanisms of resistance in Candida albicans. *Med Mycol*, *43*(4), 285-318. https://doi.org/10.1080/13693780500138971

Arastehfar, A., Daneshnia, F., Hilmioğlu-Polat, S., Fang, W., Yaşar, M., Polat, F., Metin, D. Y., Rigole, P., Coenye, T., Ilkit, M., Pan, W., Liao, W., Hagen, F., Kostrzewa, M., Perlin, D. S., Lass-Flörl, C., & Boekhout, T. (2020). First Report of Candidemia Clonal Outbreak Caused by Emerging Fluconazole-Resistant Candida parapsilosis Isolates Harboring Y132F and/or Y132F+K143R in Turkey. *Antimicrob Agents Chemother*, *64*(10). https://doi.org/10.1128/aac.01001-20

Arastehfar, A., Hilmioğlu-Polat, S., Daneshnia, F., Pan, W., Hafez, A., Fang, W., Liao, W., Şahbudak-Bal, Z., Metin, D. Y., Júnior, J. N. A., Ilkit, M., Perlin, D. S., & Lass-Flörl, C. (2021). Clonal Candidemia Outbreak by Candida parapsilosis Carrying Y132F in Turkey: Evolution of a Persisting Challenge. *Front Cell Infect Microbiol*, *11*, 676177. https://doi.org/10.3389/fcimb.2021.676177

Arikan-Akdagli, S., Gülmez, D., Doğan, Ö., Çerikçioğlu, N., Doluca Dereli, M., Birinci, A., Yıldıran Ş, T., Ener, B., Öz, Y., Metin, D. Y., Hilmioğlu-Polat, S., Kalkancı, A., Koç, N., Erturan, Z., & Fındık, D. (2019). First multicentre report of in vitro resistance rates in candidaemia isolates in Turkey. *J Glob Antimicrob Resist*, *18*, 230-234. https://doi.org/10.1016/j.jgar.2019.04.003

Bandara, H. M. H. N., Wood, D. L. A., Vanwonterghem, I., Hugenholtz, P., Cheung, B. P. K., & Samaranayake, L. P. (2020). Fluconazole resistance in Candida albicans is induced by Pseudomonas aeruginosa quorum sensing. *Scientific Reports*, *10*(1), 7769. https://doi.org/10.1038/s41598-020-64761-3

Begum, N., Lee, S., Portlock, T. J., Pellon, A., Nasab, S. D. S., Nielsen, J., Uhlen, M., Moyes, D. L., & Shoaie, S. (2022). Integrative functional analysis uncovers metabolic differences between Candida species. *Commun Biol*, *5*(1), 1013. https://doi.org/10.1038/s42003-022-03955-z

Begum, N., Lee, S., Portlock, T. J., Pellon, A., Nasab, S. D. S., Nielsen, J., Uhlen, M., Moyes, D. L., & Shoaie, S. (2022). Integrative functional analysis uncovers

metabolic differences between Candida species. *Communications Biology*, *5*(1), 1013. https://doi.org/10.1038/s42003-022-03955-z

Benedict, K., Richardson, M., Vallabhaneni, S., Jackson, B. R., & Chiller, T. (2017). Emerging issues, challenges, and changing epidemiology of fungal disease outbreaks. *Lancet Infect Dis*, *17*(12), e403-e411. https://doi.org/10.1016/s1473-3099(17)30443-7

Berkow, E. L., Manigaba, K., Parker, J. E., Barker, K. S., Kelly, S. L., & Rogers, P. D. (2015). Multidrug Transporters and Alterations in Sterol Biosynthesis Contribute to Azole Antifungal Resistance in Candida parapsilosis. *Antimicrob Agents Chemother*, *59*(10), 5942-5950. https://doi.org/10.1128/aac.01358-15

Bhattacharya, S., Sae-Tia, S., & Fries, B. C. (2020). Candidiasis and Mechanisms of Antifungal Resistance. *Antibiotics (Basel)*, *9*(6). https://doi.org/10.3390/antibiotics9060312

Branco, J., Miranda, I. M., & Rodrigues, A. G. (2023). Candida parapsilosis Virulence and Antifungal Resistance Mechanisms: A Comprehensive Review of Key Determinants. *J Fungi (Basel)*, *9*(1). https://doi.org/10.3390/jof9010080

Branco, J., Ola, M., Silva, R. M., Fonseca, E., Gomes, N. C., Martins-Cruz, C., Silva, A. P., Silva-Dias, A., Pina-Vaz, C., Erraught, C., Brennan, L., Rodrigues, A. G., Butler, G., & Miranda, I. M. (2017). Impact of ERG3 mutations and expression of ergosterol genes controlled by UPC2 and NDT80 in Candida parapsilosis azole resistance. *Clin Microbiol Infect*, *23*(8), 575.e571-575.e578. https://doi.org/10.1016/j.cmi.2017.02.002

Brandt, P., Garbe, E., & Vylkova, S. (2020). Catch the wave: Metabolomic analyses in human pathogenic fungi. *PLoS Pathog*, *16*(8), e1008757. https://doi.org/10.1371/journal.ppat.1008757

Cao, Y., Zhu, Z., Chen, X., Yao, X., Zhao, L., Wang, H., Yan, L., Wu, H., Chai, Y., & Jiang, Y. (2013). Effect of amphotericin B on the metabolic profiles of Candida albicans. *J Proteome Res*, *12*(6), 2921-2932. https://doi.org/10.1021/pr4002178

Castanheira, M., Deshpande, L. M., Messer, S. A., Rhomberg, P. R., & Pfaller, M. A. (2020). Analysis of global antifungal surveillance results reveals predominance of Erg11 Y132F alteration among azole-resistant Candida parapsilosis and Candida tropicalis and country-specific isolate dissemination. *Int J Antimicrob Agents*, *55*(1), 105799. https://doi.org/10.1016/j.ijantimicag.2019.09.003

Choi, Y. J., Kim, Y. J., Yong, D., Byun, J. H., Kim, T. S., Chang, Y. S., Choi, M. J., Byeon, S. A., Won, E. J., Kim, S. H., Shin, M. G., & Shin, J. H. (2018). Fluconazole-Resistant Candida parapsilosis Bloodstream Isolates with Y132F Mutation in ERG11 Gene, South Korea. *Emerg Infect Dis*, *24*(9), 1768-1770. https://doi.org/10.3201/eid2409.180625

Christensson, B., Sigmundsdottir, G., & Larsson, L. (1999a). D-arabinitol--a marker for invasive candidiasis. *Med Mycol*, *37*(6), 391-396. https://doi.org/10.1046/j.1365-280x.1999.00249.x

Christensson, B., Sigmundsdottir, G., & Larsson, L. (1999b). D-arabinitol — a marker for invasive candidiasis. *Medical Mycology*, *37*(6), 391-396. https://doi.org/10.1046/j.1365-280X.1999.00249.x

CLSI, M.-S. (2013). *Reference Method for Broth Dilution Antifungal Susceptibility Testing of Yeasts* (Vol. 4th ed. CLSI standard M27). Clinical and Laboratory Standards Institute.

Corzo-Leon, D. E., Peacock, M., Rodriguez-Zulueta, P., Salazar-Tamayo, G. J., & MacCallum, D. M. (2021). General hospital outbreak of invasive candidiasis due to azole-resistant Candida parapsilosis associated with an Erg11 Y132F mutation. *Med Mycol*, *59*(7), 664-671. https://doi.org/10.1093/mmy/myaa098

Costa-de-Oliveira, S., & Rodrigues, A. G. (2020). Candida albicans Antifungal Resistance and Tolerance in Bloodstream Infections: The Triad Yeast-Host-Antifungal. *Microorganisms*, *8*(2), 154. https://www.mdpi.com/2076-2607/8/2/154

Cuéllar-Cruz, M., López-Romero, E., Villagómez-Castro, J. C., & Ruiz-Baca, E. (2012). Candida species: new insights into biofilm formation. *Future Microbiol*, *7*(6), 755-771. https://doi.org/10.2217/fmb.12.48

Daneshnia, F., de Almeida Júnior, J. N., Ilkit, M., Lombardi, L., Perry, A. M., Gao, M., Nobile, C. J., Egger, M., Perlin, D. S., Zhai, B., Hohl, T. M., Gabaldón, T., Colombo, A. L., Hoenigl, M., & Arastehfar, A. (2023). Worldwide emergence of fluconazole-resistant Candida parapsilosis: current framework and future research roadmap. *Lancet Microbe*, *4*(6), e470-e480. https://doi.org/10.1016/s2666-5247(23)00067-8

Daneshnia, F., Hilmioğlu Polat, S., Ilkit, M., Shor, E., de Almeida Júnior, J. N., Favarello, L. M., Colombo, A. L., Arastehfar, A., & Perlin, D. S. (2022). Determinants of fluconazole resistance and the efficacy of fluconazole and

milbemycin oxim combination against Candida parapsilosis clinical isolates from Brazil and Turkey. *Front Fungal Biol*, *3*, 906681. https://doi.org/10.3389/ffunb.2022.906681

Demirci-Duarte, S., Arikan-Akdagli, S., & Gülmez, D. (2021). Species distribution, azole resistance and related molecular mechanisms in invasive Candida parapsilosis complex isolates: Increase in fluconazole resistance in 21 years. *Mycoses*, *64*(8), 823-830. https://doi.org/10.1111/myc.13296

Dunkel, N., Liu, T. T., Barker, K. S., Homayouni, R., Morschhäuser, J., & Rogers, P. D. (2008). A gain-of-function mutation in the transcription factor Upc2p causes upregulation of ergosterol biosynthesis genes and increased fluconazole resistance in a clinical Candida albicans isolate. *Eukaryot Cell*, *7*(7), 1180-1190. https://doi.org/10.1128/ec.00103-08

Dupont, S., Lemetais, G., Ferreira, T., Cayot, P., Gervais, P., & Beney, L. (2012). Ergosterol biosynthesis: a fungal pathway for life on land? *Evolution*, *66*(9), 2961-2968. https://doi.org/10.1111/j.1558-5646.2012.01667.x

Escribano, P., & Guinea, J. (2022). Fluconazole-resistant Candida parapsilosis: A new emerging threat in the fungi arena. *Frontiers in Fungal Biology*, *3*. https://doi.org/10.3389/ffunb.2022.1010782

Faria-Ramos, I., Neves-Maia, J., Ricardo, E., Santos-Antunes, J., Silva, A. T., Costa-de-Oliveira, S., Cantón, E., Rodrigues, A. G., & Pina-Vaz, C. (2014). Species distribution and in vitro antifungal susceptibility profiles of yeast isolates from invasive infections during a Portuguese multicenter survey. *Eur J Clin Microbiol Infect Dis*, *33*(12), 2241-2247. https://doi.org/10.1007/s10096-014-2194-8

Fekkar, A., Blaize, M., Bouglé, A., Normand, A. C., Raoelina, A., Kornblum, D., Kamus, L., Piarroux, R., & Imbert, S. (2021). Hospital outbreak of fluconazole-resistant Candida parapsilosis: arguments for clonal transmission and long-term persistence. *Antimicrob Agents Chemother*, *65*(5). https://doi.org/10.1128/aac.02036-20

Feng, W., Yang, J., Xi, Z., Ji, Y., Zhu, X., Yang, L., & Ma, Y. (2019). Regulatory Role of ERG3 and Efg1 in Azoles-Resistant Strains of Candida albicans Isolated from Patients Diagnosed with Vulvovaginal Candidiasis. *Indian J Microbiol*, *59*(4), 514-524. https://doi.org/10.1007/s12088-019-00833-x

Flowers, S. A., Barker, K. S., Berkow, E. L., Toner, G., Chadwick, S. G., Gygax, S. E., Morschhäuser, J., & Rogers, P. D. (2012). Gain-of-function mutations in UPC2

are a frequent cause of ERG11 upregulation in azole-resistant clinical isolates of Candida albicans. *Eukaryot Cell*, *11*(10), 1289-1299. https://doi.org/10.1128/ec.00215-12

Flowers, S. A., Colón, B., Whaley, S. G., Schuler, M. A., & Rogers, P. D. (2015). Contribution of clinically derived mutations in ERG11 to azole resistance in Candida albicans. *Antimicrob Agents Chemother*, *59*(1), 450-460. https://doi.org/10.1128/aac.03470-14

Franconi, I., Rizzato, C., Poma, N., Tavanti, A., & Lupetti, A. (2023). Candida parapsilosis sensu stricto Antifungal Resistance Mechanisms and Associated Epidemiology. *J Fungi (Basel)*, *9*(8). https://doi.org/10.3390/jof9080798

Gallo-Ebert, C., Donigan, M., Stroke, I. L., Swanson, R. N., Manners, M. T., Francisco, J., Toner, G., Gallagher, D., Huang, C. Y., Gygax, S. E., Webb, M., & Nickels, J. T., Jr. (2014). Novel antifungal drug discovery based on targeting pathways regulating the fungus-conserved Upc2 transcription factor. *Antimicrob Agents Chemother*, *58*(1), 258-266. https://doi.org/10.1128/aac.01677-13

Gallo, M., Giovati, L., Magliani, W., Pertinhez, T. A., Conti, S., Ferrari, E., Spisni, A., & Ciociola, T. (2022). Metabolic Plasticity of Candida albicans in Response to Different Environmental Conditions. *J Fungi (Basel)*, *8*(7). https://doi.org/10.3390/jof8070723

Gallo, M., Giovati, L., Magliani, W., Pertinhez, T. A., Conti, S., Ferrari, E., Spisni, A., & Ciociola, T. (2022). Metabolic Plasticity of Candida albicans in Response to Different Environmental Conditions. *Journal of Fungi*, *8*(7), 723. https://www.mdpi.com/2309-608X/8/7/723

Garcia-Rubio, R., de Oliveira, H. C., Rivera, J., & Trevijano-Contador, N. (2019). The Fungal Cell Wall: Candida, Cryptococcus, and Aspergillus Species. *Front Microbiol*, *10*, 2993. https://doi.org/10.3389/fmicb.2019.02993

Guinea, J. (2014). Global trends in the distribution of Candida species causing candidemia. *Clin Microbiol Infect*, *20 Suppl 6*, 5-10. https://doi.org/10.1111/1469-0691.12539

Hornby, J. M., & Nickerson, K. W. (2004). Enhanced production of farnesol by Candida albicans treated with four azoles. *Antimicrob Agents Chemother*, *48*(6), 2305-2307. https://doi.org/10.1128/aac.48.6.2305-2307.2004

Katragkou, A., Alexander, E. L., Eoh, H., Raheem, S. K., Roilides, E., & Walsh, T. J. (2016). Effects of fluconazole on the metabolomic profile of Candida albicans. *J Antimicrob Chemother*, *71*(3), 635-640. https://doi.org/10.1093/jac/dkv381

Kayingo, G., & Wong, B. (2005). The MAP kinase Hog1p differentially regulates stress-induced production and accumulation of glycerol and d-arabitol in Candida albicans. *Microbiology*, *151*(9), 2987-2999. https://doi.org/https://doi.org/10.1099/mic.0.28040-0

Khalifa, H. O., Watanabe, A., & Kamei, K. (2024). Antifungal Resistance and Genotyping of Clinical Candida parapsilosis Complex in Japan. *Journal of Fungi*, *10*(1), 4. https://www.mdpi.com/2309-608X/10/1/4

Kim, H. S., & Fay, J. C. (2007). Genetic variation in the cysteine biosynthesis pathway causes sensitivity to pharmacological compounds. *Proceedings of the National Academy of Sciences*, *104*(49), 19387-19391. https://doi.org/doi:10.1073/pnas.0708194104

MacPherson, S., Akache, B., Weber, S., Deken, X. D., Raymond, M., & Turcotte, B. (2005). Candida albicans Zinc Cluster Protein Upc2p Confers Resistance to Antifungal Drugs and Is an Activator of Ergosterol Biosynthetic Genes. *Antimicrobial Agents and Chemotherapy*, *49*(5), 1745-1752. https://doi.org/doi:10.1128/aac.49.5.1745-1752.2005

Madji Hounoum, B., Blasco, H., Nadal-Desbarats, L., Diémé, B., Montigny, F., Andres, C. R., Emond, P., & Mavel, S. (2015). Analytical methodology for metabolomics study of adherent mammalian cells using NMR, GC-MS and LC-HRMS. *Anal Bioanal Chem*, *407*(29), 8861-8872. https://doi.org/10.1007/s00216-015-9047-x

Magobo, R. E., Lockhart, S. R., & Govender, N. P. (2020). Fluconazole-resistant Candida parapsilosis strains with a Y132F substitution in the ERG11 gene causing invasive infections in a neonatal unit, South Africa. *Mycoses*, *63*(5), 471-477. https://doi.org/10.1111/myc.13070

Martini, C., Torelli, R., de Groot, T., De Carolis, E., Morandotti, G. A., De Angelis, G., Posteraro, B., Meis, J. F., & Sanguinetti, M. (2020). Prevalence and Clonal Distribution of Azole-Resistant Candida parapsilosis Isolates Causing Bloodstream Infections in a Large Italian Hospital. *Front Cell Infect Microbiol*, *10*, 232. https://doi.org/10.3389/fcimb.2020.00232

Morio, F., Pagniez, F., Lacroix, C., Miegeville, M., & Le Pape, P. (2012). Amino acid substitutions in the Candida albicans sterol Δ5,6-desaturase (Erg3p) confer azole resistance: characterization of two novel mutants with impaired virulence. *J Antimicrob Chemother*, *67*(9), 2131-2138. https://doi.org/10.1093/jac/dks186

Morschhäuser, J. (2016). The development of fluconazole resistance in Candida albicans – an example of microevolution of a fungal pathogen. *Journal of Microbiology*, *54*(3), 192-201. https://doi.org/10.1007/s12275-016-5628-4

Murray, P. R., Rosenthal, K., & Pfaller, M. A. (2020). *Medical Microbiology: Medical Microbiology E-Book*. Elsevier Health Sciences.

Nucci, M., Queiroz-Telles, F., Alvarado-Matute, T., Tiraboschi, I. N., Cortes, J., Zurita, J., Guzman-Blanco, M., Santolaya, M. E., Thompson, L., Sifuentes-Osornio, J., Echevarria, J. I., & Colombo, A. L. (2013). Epidemiology of candidemia in Latin America: a laboratory-based survey. *PLoS One*, *8*(3), e59373. https://doi.org/10.1371/journal.pone.0059373

Pappas, P. G., Kauffman, C. A., Andes, D. R., Clancy, C. J., Marr, K. A., Ostrosky-Zeichner, L., Reboli, A. C., Schuster, M. G., Vazquez, J. A., Walsh, T. J., Zaoutis, T. E., & Sobel, J. D. (2016). Clinical Practice Guideline for the Management of Candidiasis: 2016 Update by the Infectious Diseases Society of America. *Clin Infect Dis*, *62*(4), e1-50. https://doi.org/10.1093/cid/civ933

Parkhitko, A. A., Jouandin, P., Mohr, S. E., & Perrimon, N. (2019). Methionine metabolism and methyltransferases in the regulation of aging and lifespan extension across species. *Aging Cell*, *18*(6), e13034. https://doi.org/10.1111/acel.13034

Pfaller, M. A., & Diekema, D. J. (2012). Progress in antifungal susceptibility testing of Candida spp. by use of Clinical and Laboratory Standards Institute broth microdilution methods, 2010 to 2012. *J Clin Microbiol*, *50*(9), 2846-2856. https://doi.org/10.1128/jcm.00937-12

Robbins, N., Caplan, T., & Cowen, L. E. (2017). Molecular Evolution of Antifungal Drug Resistance. *Annu Rev Microbiol*, *71*, 753-775. https://doi.org/10.1146/annurev-micro-030117-020345

Rossignol, T., Logue, M. E., Reynolds, K., Grenon, M., Lowndes, N. F., & Butler, G. (2007). Transcriptional response of Candida parapsilosis following exposure to farnesol. *Antimicrob Agents Chemother*, *51*(7), 2304-2312. https://doi.org/10.1128/aac.01438-06

Roth, R., Madhani, H. D., & Garcia, J. F. (2018). Total RNA Isolation and Quantification of Specific RNAs in Fission Yeast. *Methods Mol Biol*, *1721*, 63-72. https://doi.org/10.1007/978-1-4939-7546-4_6

Rybak, J. M., Dickens, C. M., Parker, J. E., Caudle, K. E., Manigaba, K., Whaley, S. G., Nishimoto, A. T., Luna-Tapia, A., Roy, S., Zhang, Q., Barker, K. S., Palmer, G. E., Sutter, T. R., Homayouni, R., Wiederhold, N. P., Kelly, S. L., & Rogers, P. D. (2017). Loss of C-5 Sterol Desaturase Activity Results in Increased Resistance to Azole and Echinocandin Antifungals in a Clinical Isolate of Candida parapsilosis. *Antimicrobial Agents and Chemotherapy*, *61*(9), 10.1128/aac.00651-00617. https://doi.org/doi:10.1128/aac.00651-17

Sanglard, D., Ischer, F., Parkinson, T., Falconer, D., & Bille, J. (2003). Candida albicans mutations in the ergosterol biosynthetic pathway and resistance to several antifungal agents. *Antimicrob Agents Chemother*, *47*(8), 2404-2412. https://doi.org/10.1128/aac.47.8.2404-2412.2003

Sanglard, D., Ischer, F., Parkinson, T., Falconer, D., & Bille, J. (2003). Candida albicans Mutations in the Ergosterol Biosynthetic Pathway and Resistance to Several Antifungal Agents. *Antimicrobial Agents and Chemotherapy*, *47*(8), 2404-2412. https://doi.org/doi:10.1128/aac.47.8.2404-2412.2003

Schaefer, K., Wagener, J., Ames, R. M., Christou, S., MacCallum, D. M., Bates, S., & Gow, N. A. R. (2020). Three Related Enzymes in Candida albicans Achieve Arginine- and Agmatine-Dependent Metabolism That Is Essential for Growth and Fungal Virulence. *mBio*, *11*(4). https://doi.org/10.1128/mBio.01845-20

Schoch, C. L., Ciufo, S., Domrachev, M., Hotton, C. L., Kannan, S., Khovanskaya, R., Leipe, D., McVeigh, R., O'Neill, K., Robbertse, B., Sharma, S., Soussov, V., Sullivan, J. P., Sun, L., Turner, S., & Karsch-Mizrachi, I. (2020). NCBI Taxonomy: a comprehensive update on curation, resources and tools. *Database (Oxford)*, *2020*. https://doi.org/10.1093/database/baaa062

Silva, A. P., Miranda, I. M., Guida, A., Synnott, J., Rocha, R., Silva, R., Amorim, A., Pina-Vaz, C., Butler, G., & Rodrigues, A. G. (2011). Transcriptional Profiling of Azole-Resistant Candida parapsilosis Strains. *Antimicrobial Agents and Chemotherapy*, *55*(7), 3546-3556. https://doi.org/doi:10.1128/AAC.01127-10

Silver, P. M., Oliver, B. G., & White, T. C. (2004). Role of Candida albicans transcription factor Upc2p in drug resistance and sterol metabolism. *Eukaryot Cell*, *3*(6), 1391-1397. https://doi.org/10.1128/ec.3.6.1391-1397.2004

Song, N., Zhou, X., Li, D., Li, X., & Liu, W. (2022). A Proteomic Landscape of Candida albicans in the Stepwise Evolution to Fluconazole Resistance. *Antimicrob Agents Chemother*, *66*(4), e0210521. https://doi.org/10.1128/aac.02105-21

Soulountsi, V., Schizodimos, T., & Kotoulas, S. C. (2021). Deciphering the epidemiology of invasive candidiasis in the intensive care unit: is it possible? *Infection*, *49*(6), 1107-1131. https://doi.org/10.1007/s15010-021-01640-7

Souza, A. C., Fuchs, B. B., Pinhati, H. M., Siqueira, R. A., Hagen, F., Meis, J. F., Mylonakis, E., & Colombo, A. L. (2015). Candida parapsilosis Resistance to Fluconazole: Molecular Mechanisms and In Vivo Impact in Infected Galleria mellonella Larvae. *Antimicrob Agents Chemother*, *59*(10), 6581-6587. https://doi.org/10.1128/aac.01177-15

Tan, L., Chen, L., Yang, H., Jin, B., Kim, G., & Im, Y. J. (2022). Structural basis for activation of fungal sterol receptor Upc2 and azole resistance. *Nature Chemical Biology*, *18*(11), 1253-1262. https://doi.org/10.1038/s41589-022-01117-0

Tavanti, A., Davidson, A. D., Gow, N. A., Maiden, M. C., & Odds, F. C. (2005). Candida orthopsilosis and Candida metapsilosis spp. nov. to replace Candida parapsilosis groups II and III. *J Clin Microbiol*, *43*(1), 284-292. https://doi.org/10.1128/jcm.43.1.284-292.2005

Thomaz, D. Y., de Almeida, J. N., Jr., Lima, G. M. E., Nunes, M. O., Camargo, C. H., Grenfell, R. C., Benard, G., & Del Negro, G. M. B. (2018). An Azole-Resistant Candida parapsilosis Outbreak: Clonal Persistence in the Intensive Care Unit of a Brazilian Teaching Hospital. *Front Microbiol*, *9*, 2997. https://doi.org/10.3389/fmicb.2018.02997

Tosun, I., Akyuz, Z., Guler, N. C., Gulmez, D., Bayramoglu, G., Kaklikkaya, N., Arikan-Akdagli, S., & Aydin, F. (2013). Distribution, virulence attributes and antifungal susceptibility patterns of Candida parapsilosis complex strains isolated from clinical samples. *Medical Mycology*, *51*(5), 483-492. https://doi.org/10.3109/13693786.2012.745953

Tóth, R., Nosek, J., Mora-Montes, H. M., Gabaldon, T., Bliss, J. M., Nosanchuk, J. D., Turner, S. A., Butler, G., Vágvölgyi, C., & Gácser, A. (2019). Candida parapsilosis: from Genes to the Bedside. *Clin Microbiol Rev*, *32*(2). https://doi.org/10.1128/cmr.00111-18

van Asbeck, E. C., Clemons, K. V., & Stevens, D. A. (2009). Candida parapsilosis: a review of its epidemiology, pathogenesis, clinical aspects, typing and antimicrobial susceptibility. *Crit Rev Microbiol*, *35*(4), 283-309. https://doi.org/10.3109/10408410903213393

Wells, C. L., Sirany, M. S., & Blazevic, D. J. (1983). Evaluation of serum arabinitol as a diagnostic test for candidiasis. *Journal of Clinical Microbiology*, *18*(2), 353-357. https://doi.org/doi:10.1128/jcm.18.2.353-357.1983

White, T. C., & Silver, P. M. (2005). Regulation of sterol metabolism in Candida albicans by the UPC2 gene. *Biochemical Society Transactions*, *33*(5), 1215-1218. https://doi.org/10.1042/bst0331215

WHO. (2022). *WHO fungal priority pathogens list to guide research, development and public health action*. https://who.int/publications/i/item/9789240060241

Xiang, M.-J., Liu, J.-Y., Ni, P.-H., Wang, S., Shi, C., Wei, B., Ni, Y.-X., & Ge, H.-L. (2013). Erg11 mutations associated with azole resistance in clinical isolates of Candida albicans. *FEMS Yeast Research*, *13*(4), 386-393. https://doi.org/10.1111/1567-1364.12042

Xu, Y., Chen, L., & Li, C. (2008). Susceptibility of clinical isolates of Candida species to fluconazole and detection of Candida albicans ERG11 mutations. *Journal of Antimicrobial Chemotherapy*, *61*(4), 798-804. https://doi.org/10.1093/jac/dkn015

Yang, H., Tong, J., Lee, C. W., Ha, S., Eom, S. H., & Im, Y. J. (2015). Structural mechanism of ergosterol regulation by fungal sterol transcription factor Upc2. *Nature Communications*, *6*(1), 6129. https://doi.org/10.1038/ncomms7129

Zhou, Y., Liao, M., Zhu, C., Hu, Y., Tong, T., Peng, X., Li, M., Feng, M., Cheng, L., Ren, B., & Zhou, X. (2018). ERG3 and ERG11 genes are critical for the pathogenesis of Candida albicans during the oral mucosal infection. *International Journal of Oral Science*, *10*(2), 9. https://doi.org/10.1038/s41368-018-0013-2